CHALMERS

Numerical and Experimental Investigation of the Atkinson Cycle on a 2.0 liter 4-cylinder Turbocharged SI-engine

Master's Thesis in Automotive Engineering

Fredrik Holst
Manne Solbreck

Department of Applied Mechanics
Division of Automotive Engineering
CHALMERS UNIVERSITY OF TECHNOLOGY
Göteborg, Sweden 2014
Master's thesis 2014:49

MASTER'S THESIS IN AUTOMOTIVE ENGINEERING

Numerical and Experimental Investigation of the Atkinson Cycle on a 2.0 liter 4-cylinder Turbocharged SI-engine

FREDRIK HOLST

MANNE SOLBRECK

Department of Applied Mechanics
Division of Automotive Engineering
CHALMERS UNIVERSITY OF TECHNOLOGY

Göteborg, Sweden 2014

Numerical and Experimental Investigation of the Atkinson Cycle on a 2.0 liter 4-cylinder Turbocharged SI-engine

FREDRIK HOLST, MANNE SOLBRECK

Master's Thesis 2014:4949
ISSN 1652-8557
Department of Applied Mechanics
Division of Automotive Engineering
Chalmers University of Technology
SE-412 96 Göteborg
Sweden
Telephone: + 46 (0)31-772 1000

Department of Applied Mechanics
Göteborg, Sweden 2014

ACKNOWLEDGEMENTS

This master thesis project was initiated by and carried out at Volvo Car Corporation, a car manufacturer in Gothenburg. We would especially like to thank our supervisor at Volvo, Fredrik Ekström for his dedication, comments and guidance throughout this project. We would also like to give special thanks to our supervisor at Chalmers, Gerben Doornbos, for all his support and commitment and for helping us with comments on the report. Furthermore this project would not have been possible without the assistance and involvement from various employees at Volvo, Jens Lundmark, Håkan Sandström, Andreas Flysjö, Daniel Lundahl and Henrik Jansson. But we would especially like to express our gratitude to Lars Davidsson at Volvo for his help to sort out the practicalities throughout this project. Last but not least, we would like to thank all other people at Chalmers that in some way was involved in completing this project, especially the staff in the engine test facilities and our examiner Ingemar Denbratt. Thanks to all of you for making this an enjoyable and exciting journey.

Fredrik Holst & Manne Solbreck, Gothenburg 2014-06-17

Numerical and Experimental Investigation of the Atkinson Cycle on a 2.0 liter 4-cylinder Turbocharged SI-engine
Master's Thesis in Automotive Engineering

FREDRIK HOLST
MANNE SOLBRECK
Department of Applied Mechanics
Division of Automotive Engineering
Chalmers University of Technology

ABSTRACT

A realization of the Atkinson cycle provides a way of increasing fuel efficiency through an over-expansion. One way of achieving an over-expanded cycle is through the implementation of Late Intake Valve Closing (LIVC). The aim of this master thesis is therefore to investigate LIVC as a strategy towards improving fuel efficiency. The research includes a numerical study with simulations performed in GT-power, but also an experimental study where tests were performed on a Volvo 2.0 liter 4-cylinder turbocharged SI-engine. This was done for the purpose of verifying the findings from the simulations.

For the numerical study, different intake valve closings between 60 and 100 crank angle degrees after bottom dead center were simulated in GT-power with respect to decreased break specific fuel consumption (BSFC). The effects of varying the valve lift were also investigated. Simulations were also performed with increased geometric compression ratio to compensate for the decreased effective compression ratio caused by LIVC. The simulation results suggest that BSFC could be reduced with 7-8% over a wide range of loads and engine speeds.

The baseline engine was modified with a new intake camshaft and new pistons in order to be consistent with the simulated engine. An experimental study of the modified engine was then performed and instead of the 7-8% BSFC reduction suggested by the simulations, the experimental results showed a 2-6% reduction of BSFC. This was found for engine speeds up to 2100 rpm and loads up to 8-9 bar. At 3000 rpm the BSFC was instead increased which was an unexpected outcome that deviates from what the simulations suggested. This is believed to be partly caused by increased pumping losses at this engine speed as a consequence of high back pressure in the exhaust manifold.

Key words: Atkinson cycle, late intake valve closing, LIVC, Miller cycle, BSFC, fuel efficiency, thermal efficiency, compression ratio, expansion ratio, over-expansion, over-expanded cycle, pumping losses

Table of contents

Table of contents 1

List of abbreviations 3

1. Introduction 5

1.1 Background 5

1.2 Purpose and goal 6

1.3 Scope/Limitations 6

2. Theory/Literature review 7

2.1 Fundamental concepts of internal combustion engines 7

2.1.1 Compression & Expansion ratio 7

2.1.2 Specific fuel consumption (SFC) 7

2.1.3 Engine efficiency 8

2.2 Otto-cycle 8

2.3 Atkinson-cycle 9

2.3.1 Miller cycle 10

2.3.2 Early Intake Valve Closing (EIVC) 11

2.3.3 Late Intake Valve Closing (LIVC) 11

2.3.4 Analysis of the ideal Atkinson cycle 12

2.4 Valvetrain 15

2.4.1 Valvetrain mechanics and geometry 15

2.4.2 Valve events and gas exchange 17

2.4.3 Camshaft design limitations due to production constraints 18

2.5 Combustion in SI-engines 19

2.5.1 Ignition timing 19

2.5.2 Engine knock 20

2.5.3 Cycle-to-cycle variations 20

2.5 Effects of increasing geometric CR through piston modifications 21

2.6 Boosted operation with LIVC 21
3. Method 23
3.1 Simulation in GT-Power 23
3.1.1 Intake camshaft simulations 25
3.1.2 Compression ratio 26
3.1.3 Estimating fuel consumption using BSFC-maps 27
3.2 Hardware design 29
3.2.1 Camshaft design 29
3.2.2 Hardware design, Pistons 31
3.2.3 Simulation with complete hardware design 31
3.3 Physical testing 32
3.3.1Engine rig and test equipment 32
4. Results 36
4.1 Simulation results 36
4.1.1 Effects found from increasing IV duration 36
4.1.2 Effects found from altering the valve lift 39
4.1.3 Compression ratio 40
4.1.4 Estimated fuel consumption 42
4.1.5 Comparison of simulation results for baseline engine and modified engine 43
4.2 Experimental results from engine tests 46
5. Discussion 51
5.1 Simulations 51
5.2 Engine tests 52
6. Conclusions 54
7. References 55
Appendix A. Official engine data 56
Appendix B. Testing results, Emissions 57

List of abbreviations

aBDC	After bottom dead center
aTDC	After top dead center
BDC	Bottom dead center
BMEP	Break mean effective pressure
BSFC	Break specific fuel consumption
CAD	Crank angle degrees
CR	Compression ratio
EGT	Exhaust gas temperature
EIVC	Early intake valve closing
EP	Entry performance
ER	Expansion ratio
EV	Exhaust valve
EVC	Exhaust valve closing
EVO	Exhaust valve opening
IMEP	Indicated mean effective pressure
IV	Intake valve
IVC	Intake valve closing
IVO	Intake valve opening
LIVC	Late intake valve closing
LP	Low performance
MAP	Manifold air pressure
MAT	Manifold air temperature
MBT	Maximum break torque timing
MP	Medium performance
PMEP	Pumping mean effective pressure
RPM	Revolutions per minute
TDC	Top dead center
TDCf	Top dead center firing
TDCnf	Top dead center not firing
VCC	Volvo Car Corporation
VVT	Variable valve timing
WOT	Wide open throttle

1. Introduction

This chapter will give an introduction to the thesis starting with a description of the background to the project. Then the purpose of the thesis will be described and finally the scope of the thesis will be described, including limitations that define the boundaries of what has been investigated.

1.1 Background

There are currently above one billion passenger cars in traffic around the world. By the year 2050 this number is expected to increase to two billion cars. This growth has a large environmental impact and has led governments around the world to request more stringent demands regarding emissions. Vehicle manufacturers are therefore struggling to reduce CO_2 emissions of the future fleet. Also environmentally conscious customers start to demand lower emissions and better fuel economy. Over the last decades, lots of focus has been put into examining different ways of improving fuel efficiency. Downsizing the engine displacement in combination with increased boost pressure has been a popular method to achieve better fuel economy. This effectively switches the operation point in the engine's load map towards higher loads which moves the operating point to an area with higher efficiency. But there are also other ways of achieving improved fuel efficiency.

Looking back at the mid-19th century, an inventor named James Atkinson discovered a way of achieving improved fuel consumption through utilization of an over-expanded cycle. By separating the compression ratio from the expansion ratio he achieved a longer power stroke than compression stroke which ultimately resulted in higher fuel efficiency compared to a conventional engine. The drawback of Atkinson's engine was a low power density. A large displacement volume was required in order to achieve a satisfying power output which made his engine heavy. Atkinson's brilliant concept was therefore overshadowed by the more power dense Otto engine and eventually it was forgotten.

In the mid-20th century an inventor named Ralph Miller discovered a way of utilizing Atkinson's cycle by using the valve events. By closing the intake valves well before the piston reaches bottom dead center the effective displacement and effective compression is reduced in size. Consequently the expansion stroke is longer than the compression stroke which enables an over-expansion. This strategy of early valve closing is known as Early Intake Valve Closing (EIVC). The same effect is realized by adopting Late Intake Valve Closing (LIVC). The intake valves are then closed well after the piston has passed bottom dead center. A portion of the charge air is then pushed back into the intake manifold resulting in a shorter compression stroke than expansion stroke. During the past decade these strategies for improving fuel efficiency have been investigated by various car manufacturers such as Toyota, Mazda, Nissan and Ford. Over-expanded cycles are currently interesting for hybrid applications where the lower power density is compensated for by electric motors. Currently, car models such as the Toyota Prius and Mazda's skyactiv-G family utilize LIVC for fuel efficiency improvements. Volvo Car Corporation (VCC) now wishes to initiate an investigation of Atkinson's cycle as a strategy for future fuel efficiency improvements.

1.2 Purpose and goal

The purpose of this project is to investigate Late Intake Valve Closing (LIVC) as a strategy for improving fuel efficiency. The study consists of two parts where the first part involves a numerical study and the second part involves an experimental investigation in order to confirm the findings from the numerical study. The engine used for the project is a Volvo 2.0 liter 4-cylinder turbocharged SI-engine.

The goal of the numerical study is to provide a suggestion of how the original engine should be modified in order to improve fuel efficiency using LIVC. The proposed modifications should then be confirmed in the experimental investigation through tests in an engine test rig and evaluated against test data from the baseline engine. A second part of the goal for this project is to implement the proposed modifications in a cost efficient way by using hardware already available at VCC.

1.3 Scope/Limitations

- Only LIVC is investigated in this project. EIVC is therefore not evaluated nor compared to LIVC regarding its capacity to improve fuel efficiency.
- Even though the literature study reveals that a supercharger is beneficial to increase boost pressure with LIVC, it was decided upon the project start that a turbocharger was going to be used. It was decided before the project started that the turbo used for Volvo's low- and entry performance (LP/EP) models was going to be used for the experimental study. The effects from using a supercharger as well as from using other turbines are therefore not investigated since it is outside the scope of this project.
- During the early part of the project a brief examination of different durations for the exhaust camshaft was performed. This showed almost no efficiency improvement or in some cases deterioration of fuel efficiency. It was therefore decided in an early stage of the project that the exhaust camshaft from the baseline engine was going to be used for the experimental study. A thorough investigation of how shorter or longer exhaust cam duration would affect the end result is therefore not provided in this project.
- The effects from changing the geometric compression ratio are investigated during the numerical study. The simulations are performed without adjustments of the simulation model to compensate for changes of the combustion chamber geometry. Effects from increased heat losses due to higher surface to volume ratio or changes of the in-cylinder charge motion are therefore not investigated numerically. Decisions regarding compression ratio for the LIVC-engine are therefore, although supported with data, taken partially based on estimations and expectations.
- Only steady state operation is considered in this project. Transient behavior due to the lower trapped volume and due to hardware changes within the boost system is therefore not investigated in this thesis work.
- Emissions are measured during testing but will not be thoroughly evaluated and discussed as in why it might differ from the emissions of the baseline engine. It is almost merely presented due to interest for future research.

2. Theory/Literature review

This thesis work is about an investigation of the Atkinson cycle which includes computer simulations as well as physical testing on a Volvo engine. It is therefore vital to describe some fundamental theory of Atkinson's cycle and how it differs from the conventional Otto cycle. But also to state what has been done in previous research and how it has been embraced into today's production vehicles.

In this project, Atkinson's cycle was implemented through Late Intake Valve Closing (LIVC). Theory around the valvetrain and its components are therefore necessary which also includes the different valve events effect on the gas exchange process. The valvetrain section is then followed by theory concerning the combustion process in SI-engines. This aims at explaining parameters and target values that had to be considered.

2.1 Fundamental concepts of internal combustion engines

This section provides a description of fundamental concepts of internal combustion engines that have been useful throughout this project. Different ways of defining the compression ratio as well as the expansion ratio is provided. From this follows a definition of specific fuel consumption and engine efficiency.

2.1.1 Compression & Expansion ratio

The geometric compression ratio (CR) is defined as the maximum cylinder volume divided by the minimum cylinder volume. The minimum cylinder volume is known as the clearance volume, V_c. The maximum cylinder volume is then equal to the displaced volume, V_d, plus the clearance volume which generates equation (2.1) for geometric compression ratio.

$$r_c = \frac{V_d + V_c}{V_c} \qquad (2.1)$$

The expansion ratio follows the same relation as the geometric CR which means that in a conventional Otto engine the relationship between expansion and compression has a 1:1 ratio. In a real engine, Intake Valve Closing (IVC) does not occur at BDC but usually some degrees after. From this it follows that the actual CR, also known as the effective CR, differentiates from the geometric CR. Later closing of the intake valves consequently results in reduced effective CR and a longer expansion stroke than compression stroke which is fundamental in order to achieve Atkinson's cycle with LIVC.

2.1.2 Specific fuel consumption (SFC)

The specific fuel consumption is a measure of how efficiently the engine uses the supplied fuel to produce work. When one performs engine tests the fuel mass flow and power output is measured. These parameters relates to specific fuel consumption according to:

$$sfc = \frac{\dot{m}_f}{P} \quad [g/kWh] \qquad (2.2)$$

This relation could be used to relate the fuel mass flow to the indicated power, i.e. neglecting mechanical friction losses, or it could be related to the break power which includes mechanical losses. This gives the indicated specific fuel consumption (ISFC) and break specific fuel consumption (BSFC) respectively. It should be noted that this is not a fuel consumption measure but rather an efficiency measure.

2.1.3 Engine efficiency

There are several ways of defining the efficiency of a combustion engine and how it is defined depends on what efficiency measure one wants to look at. Only a portion of the injected fuel energy is used to produce work on the piston. How much of the fuel energy that is used to produce work is denoted by the thermal efficiency. This includes pumping losses during the intake and exhaust stroke but excludes mechanical losses due to friction. The thermal efficiency is a thermodynamic efficiency measure which assumes that all the energy of the injected fuel is released during combustion. However, in a real engine, a small portion of the fuel energy is not released during combustion. For mixtures richer than stoichiometric a lack of oxygen prevents complete combustion and a part of the injected fuel will also remain in crevices within the combustion chamber. The fraction of heat that is released from the injected fuel is denoted by the combustion efficiency. The fuel conversion efficiency is defined as the product of the thermal and combustion efficiency and provides an efficiency measure of the combustion. If the mechanical losses are taken into consideration one gets a measure of the engine's total efficiency. This measure explains the fraction of the injected fuel energy that is used to produce the output work on the crankshaft and it is defined as follows:

$$\eta_{tot} = \frac{1}{BSFC \cdot Q_{HV}} \qquad (2.3)$$

Q_{HV} denotes the fuel's heating value and throughout this thesis, the lower heating value will be used.

2.2 Otto-cycle

The Otto-cycle is the thermodynamic cycle which is used in conventional gasoline four stroke engines. In an Otto engine the piston is mechanically linked to the crankshaft through the connecting rod which imposes that the piston's upward stroke and downward stroke is of equal length. IVO and IVC occur around TDC and BDC respectively and the other way around for the exhaust valve events. Since the upward stroke and downward stroke are of equal length, this makes the compression ratio approximately equal to the expansion ratio. At the end of the expansion stroke the cylinder pressure is still relatively high, especially for high loads. A cranktrain design that allows further expansion would have been able to use the excess pressure to produce work on the piston. But in the Otto engine, the excess pressure at the end of the power stroke is instead evacuated through the exhaust manifold at EVO.

The load in an Otto engine is controlled by the throttle, which effectively alters the intake pressure, and thereby the mass of air that is pulled into the cylinders. A small throttle opening causes a large pressure drop and a wide open throttle causes almost no pressure drop at all.

High intake pressure means that a larger mass of air is inducted to the engine which consequently leads to a higher volumetric efficiency. High intake pressure therefore corresponds to high load and low pressure to low load. Since the crankcase pressure is around atmospheric, intake pressures below atmospheric causes a negative work on the system, i.e. pumping losses during the intake stroke. The magnitude of the pumping losses consequently decreases with increased throttle opening.

2.3 Atkinson-cycle

The Atkinson cycle originates from a patent by James Atkinson published in 1887 [6]. It provides a way of increasing thermal efficiency through an over-expansion towards the end of the power stroke by decoupling the expansion ratio from the compression ratio. In a conventional SI engine, energy is lost when a large amount of high pressure gas is evacuated through the exhaust at EVO instead of using its availability to produce work on the piston. This residual energy towards the end of the power stroke is utilized in the Atkinson cycle to produce additional work on the piston and thereby increasing the indicated work per cycle which results in higher thermal efficiency, see *figure 1*. Atkinson's original invention achieved this mechanically through modifications of the conventional cranktrain.

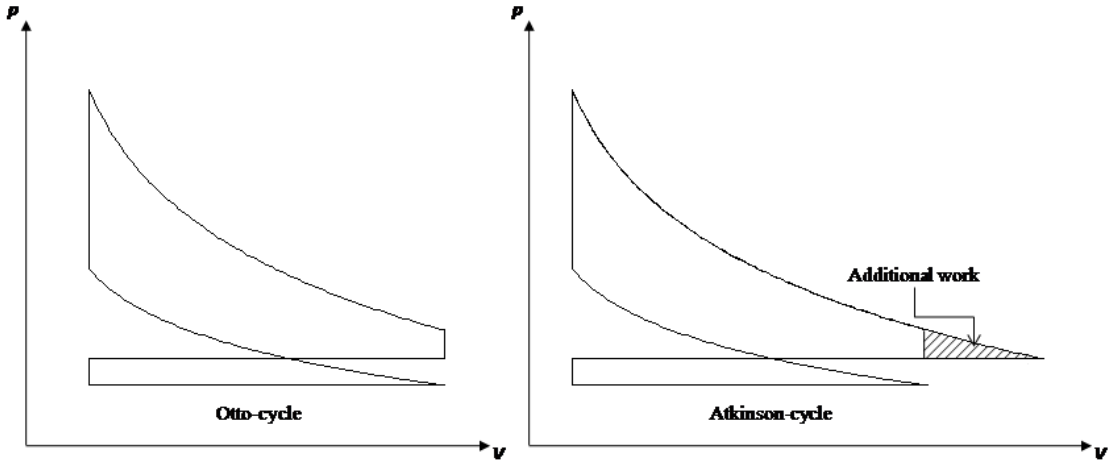

Figure 1 – pV-diagrams for the ideal Otto-cycle (left) and ideal Atkinson-cycle (right), showing the additional work obtained from the over-expansion

Atkinson's original design uses a number of additional links to achieve all four strokes of the cycle in one single rotation of the crankshaft, see *figure 2*. In a conventional engine the connecting rod is a direct link between the crankshaft and the piston. In Atkinson's design however, the connecting rod (E) is a link between the crankshaft and a solid T-end (B). The T-end (B) then connects to two other links. One of them is the piston link (A) which connects directly to the piston. The other link which is fitted to the T-end (B) is the vibrating link (C). The vibrating link moves back and forth around a fixed center pin (D) as the crankshaft completes its revolution which causes the expansion ratio to be decoupled from the compression ratio. The ratio between compression and expansion depends on the width of the T-end. In other words the center distance between the rod-ends of the vibrating link and the

piston link. The decoupling of expansion and compression imposes an over-expansion, meaning a longer power stroke than compression stroke which increases the thermal efficiency compared to a conventional Otto-engine. Although there is a potential for improvement in thermal efficiency, the power density of Atkinson's engine is lower compared to the conventional Otto-engine since the shorter compression stroke results in less amount of trapped charge.

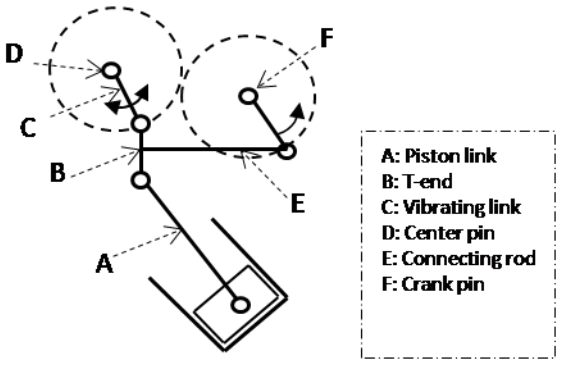

Figure 2– Atkinson engine sketch

Atkinson's original design was never embraced in production vehicles due to its complexity which made it difficult to construct the engine on a compact scale. But other ways of achieving Atkinson's principle have also been proposed [4][5][9][10] with different methods of linking the piston to the crankshaft. These include designs that are similar to Atkinson's original idea but also concepts where the piston is connected to the crankshaft through planetary gear sets. Honda proposed a design they call ExLink which stands for Extended Expansion Linkage Engine [11][12]. This system is similar to Atkinson's original design and it also benefits from low engine friction due to small angles between the connecting rod and the piston's center axis, which results in low thrust forces from the piston.

2.3.1 Miller cycle

Later on Ralph Miller proposed an alternative way of achieving an over-expanded cycle which was patented in 1957 [8]. Miller's concept utilizes a supercharged, intercooled two-stroke or four-stroke engine. The engine uses a conventional valvetrain for the air induction and exhaust evacuation but it also contains an additional valve, called compression control valve (CCV) that controls the developed pressure within the engine cylinder. The cylinder pressure is then regulated by opening the CCV which allows a certain amount of charge air to be evacuated from the cylinder during the pistons upward stroke. This ultimately changes the effective compression ratio. The amount of charge air that is evacuated depends on the valve lift of the CCV which is controlled by the intake pressure. A high intake pressure results in a higher lift and a low intake pressure results in a lower lift of the CCV valve. Subsequently a low effective compression ratio is obtained for high load operation and a high effective compression ratio for low load operation.

Although Miller was the first one who used valve events to achieve the Atkinson cycle, there have been many followers that have adopted this idea. Nowadays using valve timing to achieve Atkinson's cycle is widely adopted in hybrid vehicle applications such as the Toyota

Prius where an electric motor compensates for the power loss caused by the lower amount of trapped charge. The first car manufacturer to use the Miller cycle in a non-hybrid application was Mazda [15]. They applied LIVC on the Eunos 800 model already in 1995 which carries a supercharged 3.0 liter V6 engine developed between 1987 and 1993. Their current gasoline engines in the sky-G family also utilizes Atkinson's cycle through LIVC [14].

Volvo AB has also adopted Millers concept of using valve timing to achieve Atkinson's principle. They patented a concept in 1989 [13] which was developed for diesel engines. It was based on opening the exhaust valve for a short while during the compression stroke in order to evacuate a portion of the inducted charge. Reducing the amount of trapped charge that is compressed by the piston means that the effective compression ratio is reduced hence the expansion ratio will be larger than the compression ratio.

2.3.2 Early Intake Valve Closing (EIVC)

Miller established a way of providing the over-expansion of Atkinson's cycle without mechanical modifications of the cranktrain. One way of achieving this is through early intake valve closing (EIVC). In this case the intake valve closes during the intake stroke, well before the piston reaches BDC. After IVC the cylinder pressure will fall as the piston moves towards BDC which means that the piston has to perform work to expand the gases. This work will be almost entirely recovered during the beginning of the compression stroke as the piston moves towards TDC. The reason for this is that once the intake valve is closed the cylinder gases will act as an air spring until the piston approaches the point of IVC again and the compression begins. The negative expansion work on the piston will not be fully recovered though since heat transfer to the cylinder gases will occur between IVC and start of compression. As a consequence of all this, the effective compression ratio is reduced which results in a longer power stroke than compression stroke.

2.3.3 Late Intake Valve Closing (LIVC)

Another way of achieving Atkinson's cycle and the one being adopted in this project is Late Intake Valve Closing (LIVC). This implies that the intake valve is kept open through the intake stroke and that it closes during the compression stroke, well after the piston has passed BDC. A portion of the air which has been drawn into the cylinder is then pushed back into the intake again as the piston moves up towards TDC. Since only a part of the inducted charge is kept in the cylinder, the effective CR is reduced. This imposes a longer expansion stroke than compression stroke which means that an over-expansion will be achieved during the end of the power stroke. To achieve LIVC without moving the point of IVO, longer duration of the intake camshaft is required.

The implementation of LIVC results in increased thermal efficiency as a result of on one hand the extra work produced by the over-expansion itself, on the other hand by reduced pumping work at part load operation [1][3][4]. Since the effective displacement volume is reduced with LIVC, maintaining the mass of trapped air therefore requires that the air density is increased. This is achieved by de-throttling which then increases the intake pressure and causes a larger mass of air to be drawn into the cylinder during each intake stroke. The pumping work

reduction is a result of the increased intake pressure caused by de-throttling. Pushing back charge air into the intake before IVC causes an additional pumping work compared to a conventional engine due to the flow restriction over the valves. The contribution of this to the total pumping losses is however small compared to the pumping work reduction caused by de-throttling. The effect of an over-expanded cycle will however be a lower pressure at EVO causing less exhaust gases to be evacuated at the time of EVO. This gives a higher cylinder pressure during the first part of the exhaust stroke which slightly increases pumping work during exhaust evacuation [5].The drawback with the implementation of LIVC is that the power density will be lower compared to a conventional Otto engine. This is a consequence of the lower effective displacement volume which limits the maximum mass of trapped air.

2.3.4 Analysis of the ideal Atkinson cycle

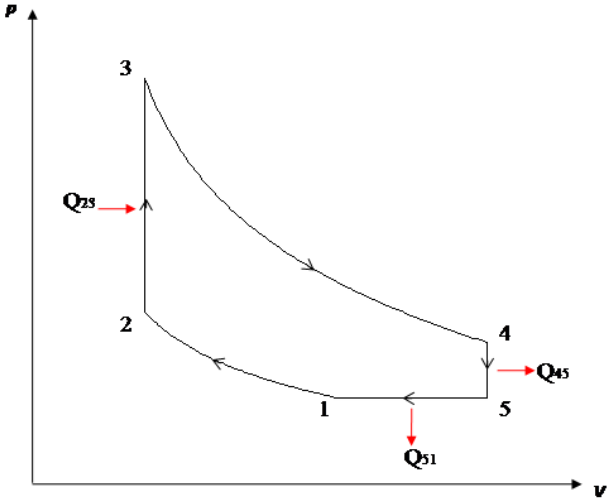

Figure 3 – pV-diagram of an ideal cycle

An investigation of the ideal Atkinson cycle shows its potential to increase thermal efficiency compared to the Otto cycle. It also reveals how thermal efficiency is affected by different ratios between expansion and compression. An ideal cycle, *figure 3*, assumes the compression stroke (1-2) to be isentropic and fully reversible. The combustion stroke (2-3) is assumed to be isochoric and adiabatic which means that all chemical energy that is released from the fuel during combustion is used to increase the temperature of the combustion gases. Consequently no heat is transferred to the surroundings. The expansion stroke (3-4) is also assumed to be isentropic and fully reversible and the exhaust valve opening (4-5) is assumed to be isochoric. Finally the exhaust evacuation (5-1) is treated as an isobaric process. Heat is supplied to the system during combustion and transferred from the system at EVO and during the exhaust stroke. The thermal efficiency of the ideal cycle is then given as:

$$\eta_{ATK} = 1 - \frac{Q_{45} + Q_{51}}{Q_{23}} = 1 - \frac{mc_v(T_4 - T_5) + mc_p(T_5 - T_1)}{mc_v(T_3 - T_2)} = 1 - \frac{(T_4 - T_5) + \gamma(T_5 - T_1)}{(T_3 - T_2)} \qquad (2.4)$$

The mixture of in-cylinder gases is assumed to have the properties of air at 25^{o}C and atmospheric pressure. The mass of the mixture is denoted m and the engine is assumed to be operated under stoichiometric conditions with air-to-fuel ratio, A/F, and specific heat ratio, γ.

The fuel is taken to be gasoline with mass, m_f, and lower heating value, Q_{LHV}. Isentropic compression gives the following relation:

$$T_2 = T_1\left(\frac{V_1}{V_2}\right)^{\gamma-1} = T_1 r_e^{\gamma-1} = T_1\left(\frac{r_g}{\sigma}\right)^{\gamma-1} \qquad (2.5)$$

Where r_e denotes the effective CR and r_g denotes the geometric CR. σ denotes the ratio between expansion and compression and therefore $\sigma = r_g/r_e$. Assuming isochoric and adiabatic combustion then gives the following relation:

$$m_f Q_{LHV} = mc_v(T_3 - T_2)$$

$$\Rightarrow \frac{T_3}{T_2} = 1 + \frac{m_f Q_{LHV}}{mc_v T_2} = 1 + \frac{m_f Q_{LHV}}{mc_v T_1 r_e^{\gamma-1}} \qquad (2.6)$$

The air/fuel ratio relation gives the following substitution for the mass of fuel:

$$\frac{m_a}{m_f} = \frac{(m - m_f)}{m_f} = \frac{A}{F}$$

$$\Rightarrow m_f = \frac{m}{1 + \frac{A}{F}} \qquad (2.7)$$

The ideal gas law gives the following equation:

$$p_1 V_1 = mRT_1 = m(\gamma - 1)c_v T_1 \qquad (2.8)$$

Combining equations (2.6), (2.7) and (2.8) results in the following temperature relation between 1-3:

$$\Rightarrow \frac{T_3}{T_2} = 1 + \frac{mQ_{LHV}}{p_1 V_1\left(1 + \frac{A}{F}\right)} \cdot \frac{\gamma - 1}{r_e^{\gamma-1}} = 1 + \frac{B(\gamma - 1)}{r_e^{\gamma-1}}$$

$$\Rightarrow \frac{T_3}{T_1} = \left(\frac{r_g}{\sigma}\right)^{\gamma-1} + B(\gamma - 1) \qquad (2.9)$$

$$B = \frac{mQ_{LHV}}{p_1 V_1\left(1 + \frac{A}{F}\right)} = \frac{Q_{LHV}\left(1 + \frac{A}{F}\right)}{RT_1} \qquad (2.10)$$

The following equation is then given by the isentropic expansion 3-4 and equation (2.9):

$$\frac{T_4}{T_3} = \left(\frac{V_3}{V_4}\right)^{\gamma-1} = \left(\frac{1}{r_g}\right)^{\gamma-1}$$

$$\Rightarrow \frac{T_4}{T_1} = \left(\frac{1}{r_g}\right)^{\gamma-1}\left[\left(\frac{r_g}{\sigma}\right)^{\gamma-1} + B(\gamma - 1)\right]$$

$$\Rightarrow \frac{T_4}{T_1} = \frac{1}{\sigma^{\gamma-1}} + \frac{B(\gamma - 1)}{\sigma^{\gamma-1} r_e^{\gamma-1}} \qquad (2.11)$$

The exhaust stroke is assumed to be an isobaric process which means that the following relationship between the temperatures in point 5 and 1 is obtained by using the ideal gas law:

$$\frac{T_5}{T_1} = \sigma \qquad (2.12)$$

Combining equations (2.4), (2.5), (2.9), (2.11) and (2.12) now gives an expression for the thermal efficiency of the ideal Atkinson cycle as follows:

$$\eta_{ATK,g} = 1 - \frac{1}{r_g^{\gamma-1}} - \frac{1 + \sigma^{\gamma}(\gamma - 1) - \gamma\sigma^{\gamma-1}}{\sigma^{\gamma-1}B(\gamma - 1)} \qquad (2.13)$$

$$\eta_{ATK,e} = 1 - \frac{1}{r_e^{\gamma-1}\sigma^{\gamma-1}} - \frac{1 + \sigma^{\gamma}(\gamma - 1) - \gamma\sigma^{\gamma-1}}{\sigma^{\gamma-1}B(\gamma - 1)} \qquad (2.14)$$

Equation (2.13) gives the graph in *figure 4*for constant geometric compression ratios between 8:1 and 14:1 and different ratios between expansion and compression, σ. Equation (2.14) gives the graph in *figure 4* for constant effective compression ratios between 8:1 and 14:1 and different ratios between expansion and compression, σ.

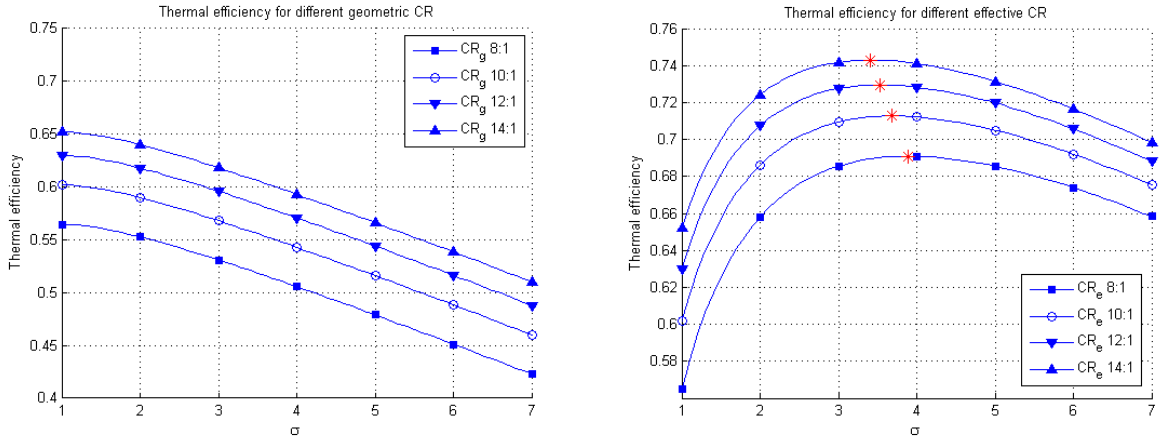

Figure 4 – Thermal efficiency over σ for constant geometric compression ratio (left) and constant effective compression ratio (right).

The curves in *figure 4 (left)*shows that the thermal efficiency has its highest value for $\sigma = 1$, which corresponds to the Otto-cycle. For this case however, the geometric compression ratio is held constant which means that the effective compression ratio is considerably reduced as σ is increased. The drop in effective CR ultimately results in reduced thermal efficiency.

In *figure 4 (right)* the effective CR is instead held constant as σ is increased. It could be observed that the thermal efficiency improves rapidly with increased σ. It could further be observed that the efficiency increases faster for lower ratios σ and that the rate of change decreases until the point of complete expansion. This point is marked with a star in *figure 4* and corresponds to the point when expansion to atmospheric pressure occurs. Further expansion beyond this point leads to a drop in thermal efficiency. In reality, the maximum expansion will be limited by the exhaust back pressure. When the effective CR is held constant one can observe theoretical efficiency improvements of around 20% compared to the Otto case.

This analysis reveals the importance of keeping sufficiently high effective CR. In practice this means that when LIVC is implemented one should compensate for the drop in effective CR by increasing the geometric CR. The analysis was made for ideal cycles without any care taken to various heat losses which is a part of the reason to why the efficiency numbers are unrealistically high. Also pumping losses during the intake and exhaust stroke was not considered in this analysis even if the main improvements with LIVC are found at part load operation. The reason for this is that this analysis was performed in order to observe the behavior with different ratios σ but also the potential of efficiency improvement with Atkinson's cycle compared to a conventional Otto-cycle.

2.4 Valvetrain

Since the implementation of LIVC requires modifications to the engine's valvetrain, a description of some aspects concerning the valvetrain is presented in this section. A brief description of the valvetrain mechanics is presented which defines and explains some parameters that have been taken into consideration when making decisions upon the camshaft specifications. The phasing of the valve lift curves has a large impact on the gas exchange processes and the amount of trapped residuals at the start of combustion. A description of how different valve timings influence the gas exchange process is therefore provided. When making decisions about camshaft specifications one also has to consider certain limitations due to the presence of various production constraints. Such limitations are provided at the end of this section.

2.4.1 Valvetrain mechanics and geometry

Valves are normally operated by double overhead camshafts that are connected to the crankshaft by either a belt or a chain. Commonly the camshafts rotate at half that of the crankshaft's speed, this is why there is a difference between cam angles and crank angles. The main components of the valvetrain are valves, springs, retainers, tappets and camshafts. The Volvo engine used for this thesis uses double overhead camshafts that are direct acting with a flat (large radius) mechanical tappet. Due to thermal expansion of the valves as the engine heats up, clearance between the tappet and the cam lobe is required which is illustrated in *figure 5* showing the profile of a cam lobe.

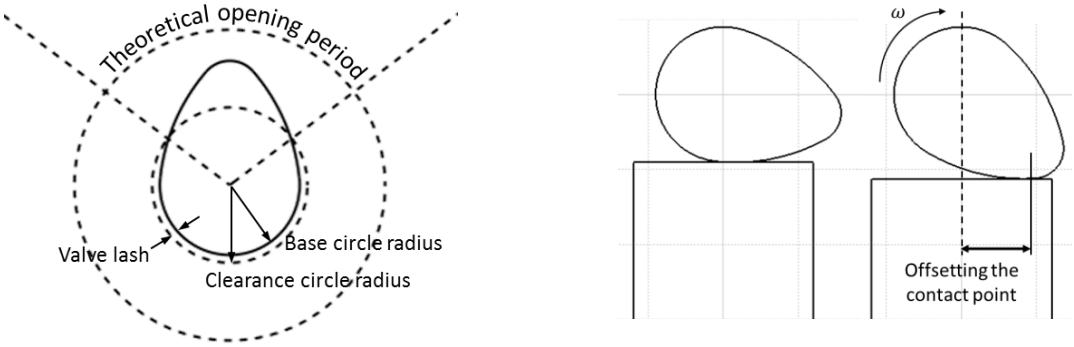

Figure 5 – Cam lobe, left figure shows the definition of different parts of the cam lobe while right figure explains how rotation offsets the contact point

The valve movement is different from the cam lobe's geometry. This is due to the fact that as the shaft turns, the point of contact between the tappet and the lobe also moves, as seen in *figure 5*. It is desirable to keep the forces within the valvetrain as low as possible in order to reduce friction and stresses of the components. This restricts the design of the cam lobes and thereby the shape of the lift curve so that the valve acceleration is kept sufficiently low.

Two terms often used to describe the valve lift curve are duration and maximum lift. The duration is usually in stated crank angles and can be specified in different ways, for instance it can be specified between the crank angles where the valve starts to lift from its seat and the crank angle where the valve is fully closed. The duration could also be specified between two crank angles where a certain lift occurs, i.e. the valve is defined as open for a certain lift for instance 1 mm. In this thesis the duration is described as the angle between the ramps since the flow is restricted during the ramps. This definition for duration is also adopted by VCC. *Figure 6* describes a lift profile with 227 CAD of duration and 8.57 mm maximum lift which is the original intake valve lift curve for the engine used in this project. The duration is marked by the two dashed black lines and IVO and IVC refers to these points.

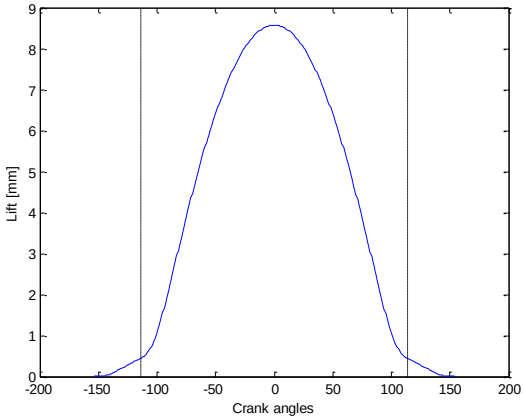

Figure 6 – Definition of IVO and IVC

The area which affects the flow is known as the effective flow area which is the area that is limited by the circumference of the valve and the valve lift. After a certain valve lift, the flow area is only limited by the diameter of the valve, see *figure 7*. Heywood [2] describes this as "Low valve lifts significantly restrict engine breathing over the mid-speed and high-speed

operating ranges. Above a critical valve lift, lift is no longer a major constraint on effective valve open area."

The engine used in this thesis has Variable Valve Timing (VVT) which allows one to phase the intake events by 50 CAD and the exhaust events by 30 CAD. Maximum lift and duration are not controllable. The VVT system in the engine used for this project uses hydraulic cam phasers which enables the engine control system to phase the intake and exhaust by applying hydraulic pressure to the phasers. At engine start up there is no oil pressure available and consequently, the intake and exhaust phases have a fixed position during engine start up.

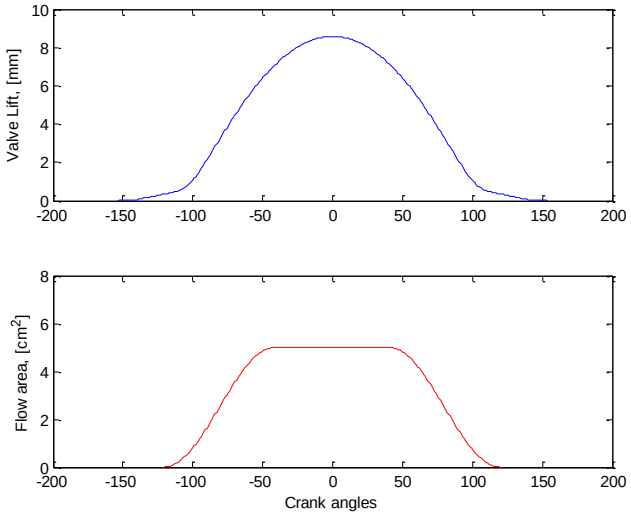

Figure 7 – Valve lift and effective flow area

2.4.2 Valve events and gas exchange

The gas exchange does not only rely on the shape of the lift curves but also on the valve timing. Different valve timings generates different benefits and drawbacks depending on engine speed and load which is why VVT is used in order to for instance increase efficiency at low engine speed or increase maximum power. *Figure 8* shows two ways of visually explaining valve timing. As can be seen in the figure there is an interval around TDC at which both valves are open at the same time. This is known as valve overlap. The valve overlap affects the scavenging and cleansing process within the cylinder, meaning that it affects the amount of trapped residuals. If the exhaust back pressure is higher than the intake pressure it causes a backflow of residuals at IVO, thus increasing the amount of trapped residuals. On the other hand, if the intake pressure is larger than the exhaust back pressure it helps the cleansing process, thus reducing the amount of trapped residuals. This is especially evident at high engine speeds where the inertia of the exhaust gases helps to accelerate the incoming fresh charge. The phenomenon is called scavenging and could be used to improve volumetric efficiency. The implementation of LIVC requires different IVC for different load points to achieve the highest possible efficiencies. Moving IVC by using VVT does however also affect IVO and therefore the overlap. At low loads the engine stability is strongly affected by the amount of trapped residuals which means that the maximum overlap is restricted for low load operation, for example at idling.

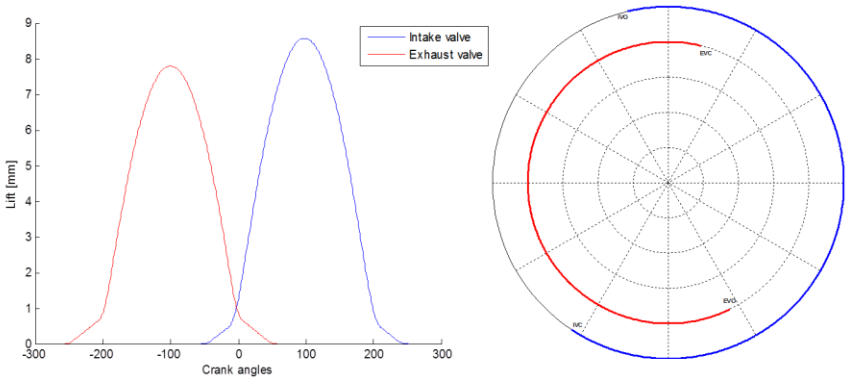

Figure 8 – Valve lift and timing explanation

Opening the intake valve too close to TDC causes the flow through the valves to be restricted during the first part of the intake stroke. This causes a negative work on the piston which could be avoided by opening the valve slightly before TDC. The same thing applies at EVO where a too late opening of the exhaust valve results in a restricted flow during the first part of the exhaust stroke.

The Intake valve is normally closed about 40-60 CAD [2] after BDC for an Otto engine which on low engine speeds can cause air to be pushed back into the manifold thus lowering the volumetric efficiency. Although on higher engine speed the inertia of the air that is moving into the cylinder becomes greater and the charging process can continue even as the compression has started and by that increasing the volumetric efficiency. This phenomenon is known as ram effect. In the same way during the exhaust stroke, the inertia of the exhaust gases at high engine speeds could cause the exhaust process to continue during the intake stroke if EVC is delayed past TDC.

2.4.3 Camshaft design limitations due to production constraints

At VCC the camshafts are manufactured by casting them close to final shape and then machining the parts that are in contact with either the tappets or the plain bearings. The outer part of the cam lobes are hardened during the casting process which means that you cannot take away too much of the material during machining. There is also a limit for the minimum amount material that needs to be removed from the cam lobes since the casted surfaces are very rough. Because of imperfections in the castings and that you cannot set the castings into the grinding machine exactly at the nominal angle, there is also an angular tolerance for the grinding machine to consider during manufacturing and design. The black outline of the cam profile in *figure 9* displays a casting of a cam lobe and the two green lines are the outer and inner tolerances. The dashed line illustrates the angular tolerance which in this figure, does not correspond to the maximum grinding depth tolerance. Tolerances can be found in *table 1*.

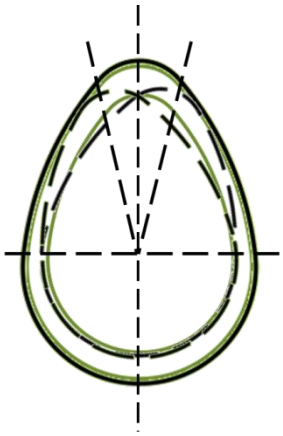

Figure 9 – Cam lobe manufacturing tolerances

Table 1 - Cam lobe manufacturing tolerances

Castings surface tolerance	±0.75mm
Castings angular tolerance	±2.4°
Grinding Angular tolerance	±1.5°
Surface hardness	>40 HRC
Maximum grinding depth	4 mm

2.5 Combustion in SI-engines

The purpose of this section is to give a brief explanation of the combustion process and to define and explain certain parameters and phenomena concerning the combustion in an SI-engine. Many parameters had to be considered in this thesis, mainly for the simulation and physical testing. Therefore this section also aims at defining target values for some parameters which have been considered throughout this project.

The combustion in an SI-engine can be divided into two main stages. The first phase is the ignition delay period or flame development phase and this is where the spark discharge occurs. The duration of the flame development period is counted from the crank angle of the spark discharge until the crank angle where 10% of the cylinder mass has burnt. The flame development period is followed by the rapid flame propagation period where the main part of the combustion occurs and consequently the largest portion of heat release. The duration of this period is usually counted between the crank angles of 10% and 90% mass fraction burnt. The burn rate is influenced by a number of factors such as ignition timing, charge motion, mixture properties, mass fraction of residuals and cylinder pressure and temperature prior to combustion.

2.5.1 Ignition timing

The combustion in an SI-engine is initiated towards the end of the compression stroke when an electrical discharge from the spark plug ignites the fuel/air mixture. The combustion thereof starts before TDC and ends in the expansion stroke a while after the point of peak cylinder pressure. The chemical energy released during compression causes a negative work transfer to the piston and the heat released after TDC gives a positive work. Advancing the

ignition too far causes excess negative work. Retarding the ignition too far and thereby delaying the combustion causes lower peak pressure and decreased output work. This also causes increased exhaust temperatures since a larger portion of the heat released from the fuel is wasted as thermal heat instead of producing work on the piston. The optimum ignition timing which gives the maximum break torque is called MBT-timing. The point where MBT is reached is affected by the burn rate and total burn duration. For optimum spark timing the peak pressure generally occurs around 10-15 CAD aTDC. It is also generally accepted that half the charge has burnt around 7-8 CAD aTDC for optimum spark timing. In order to obtain the highest efficiency values it is important to phase the combustion as close as possible to MBT timing.

2.5.2 Engine knock

Engine knock is the abnormal combustion phenomenon related to auto-ignition in front of the propagating flame. It occurs due to high local temperatures within the compressed end gases and could be avoided by enriching the mixture or by retarding ignition timing. This effectively decreases the peak pressure and therefore temperature within the combustion chamber. Consequently, engine knock limits the maximum possible ignition advance which means that MBT-timing might not be achievable for higher loads. Knock is more likely to occur at higher loads on low engine speeds than on high engine speeds. This is because at high engine speeds there is less time for heat transfer to the end gases. Also, at high engine speeds the turbulent motion increases and therefore the flame propagation is faster which enables the propagating flame to consume the end gases before auto ignition occurs. Ignition timing could therefore be further advanced at high engine speeds.

LIVC results in reduced effective CR which mitigates knock since it effectively leads to lower peak pressure and temperature during combustion. However, with LIVC there is a point in increasing the geometric CR in order to compensate for the reduced effective CR, as previously discussed. Increased geometric CR imposes a risk of knock, especially in combination with ram effects likely to occur at higher loads and engine speeds. This must be considered since the knock limit affects the maximum possible ignition advance. Too late ignition timing lowers the thermal efficiency which consequently counteracts the benefits from LIVC. Furthermore, as previously mentioned a portion of the fresh air charge is pushed back into the intake again during the compression stroke, before the intake valve closes. During its time in the cylinder it has sustained a temperature increase due to the high in-cylinder temperature. When the warm gas is pushed back to the intake it effectively results in increased intake temperature. Higher intake temperature further increases the risk of knock. Some research [3] has observed intake runner temperatures of up to 60^{o}C with LIVC.

2.5.3 Cycle-to-cycle variations

The work produced from a cylinder will not be the same each cycle. There are variations from one cycle to another which are caused by variations in turbulent charge motion, mixture composition of fuel and air but also variations in the amount of residuals within the cylinder. These variations influence the burn rate and thereby the work produced each cycle. A measure

for the size of these variations is called coefficient of variance (COV) and it denotes the IMEP standard deviation as a fraction of the average IMEP. COV is calculated as follows:

$$COV = \frac{\sigma_{imep}}{IMEP_{avg}} \qquad (2.15)$$

The burn rate is decreased by very lean or rich mixtures as well as very diluted mixtures, caused by for example too much valve overlap. This could cause incomplete flame propagation if the burn rate is heavily decreased or it could result in misfires. The presence of such phenomena could cause unstable operation primarily at low loads and idle operation where burn rate is lower. To secure stable operation, the COV should be kept below 10% [2]. For high load operation, the fastest burning cycle sets the limit of maximum ignition advance.

2.5 Effects of increasing geometric CR through piston modifications

One way of increasing the geometric CR is through modifications of the piston design. The pistons are then designed to occupy a larger part of the clearance volume at TDC. This could be achieved by simply adding material to the top of the baseline pistons. While a higher CR results in increased thermal efficiency, increasing it by means of modifications to the piston geometry give rise to certain problems that needs to be taken into consideration. Increased CR leads to higher peak pressure and causes the thrust forces from the pistons to be larger. This ultimately leads to higher friction losses and consequently reduced mechanical efficiency. Changing the geometry within the combustion chamber also affects the in-cylinder charge motion and turbulence and consequently it affects the mixing process of air and fuel vapor.

Adding material to the piston could cause a larger surface area at the piston top. Meanwhile the cylinder volume decreases which causes higher surface to volume ratios. Increased surface to volume ratio causes higher heat losses within the combustion chamber. In fact, the surface to volume ratio increases linearly with increased CR [18]. For part load operation the thermal efficiency peaks at a CR of around 15:1 and for WOT the efficiency peak occurs for a CR around 14:1 [17]. For LIVC however, the effective CR is low and approaching this limit for geometric CR is therefore not as critical as in a conventional Otto-engine.

2.6 Boosted operation with LIVC

Because of low effective displacement volume with LIVC the trapped volume of fresh charge within the cylinder is reduced compared to a conventional Otto-engine. The intake pressure therefore has to be increased in order to achieve sufficient loads. This requires a boost system which could be either a turbocharger or a supercharger.

A supercharger is usually mechanically connected to the engine cranktrain. Consequently, the obtainable boost pressure depends on engine speed. A supercharger thereby has the advantage of delivering instantaneous boost pressure without any latency time. This is positive for the transient behavior of the engine since the time to reach the desired load is reduced compared to a turbocharger. The major disadvantage with superchargers is that they impose mechanical losses due to their mechanical connection to the cranktrain which means that they require torque to deliver torque.

A turbocharger on the other hand recovers a part of the energy contained in the exhaust gases, which otherwise would be wasted, to create boost pressure. The exhaust gases accelerate a turbine wheel and due to rotational inertia of the rotating parts, it takes a certain amount of time to increase speed of the turbine wheel. This gives a latency time, also known as turbo lag. The presence of turbo lag results in a longer response time compared to a supercharger. The turbocharger is not mechanically connected to the crankshaft which means that it does not consume engine power as in the case with the supercharger. However, since it is driven by exhaust mass flow, it gives a higher back pressure in the exhaust manifold which adds to the pumping losses on the exhaust side.

The turbocharger is driven by mass flow where a higher mass flow results in higher obtainable boost pressures. Since LIVC results in lower trapped volume, it requires a higher boost pressure to achieve a certain load when it is compared to a conventional Otto-engine. It therefore requires a turbocharger that delivers high pressure ratios for low exhaust mass flows. In fact, due to the low exhaust gas volumes with LIVC, a boost system utilizing a supercharger which does not rely on exhaust gas energy would be beneficial [7][3], not least for the transient response.

3. Method

The method can be divided into several parts, and *figure 10* shows an overview of the different parts in the project. In order to estimate the effects of LIVC, basic calculations on ideal cycles were performed. The results from these are presented in the chapter *2.3.4 Analysis of the ideal Atkinson cycle*. The project continued with simulations in GT-power with a pre-existing model of Volvo's 4-cylinder petrol engine, the VEP4 MP. Different camshaft geometries and compression ratios were simulated in order to effectively implement LIVC. The result from the simulations was an intake camshaft designed for LIVC. Simulations using the final camshaft design were then performed in order to decide the geometric CR.

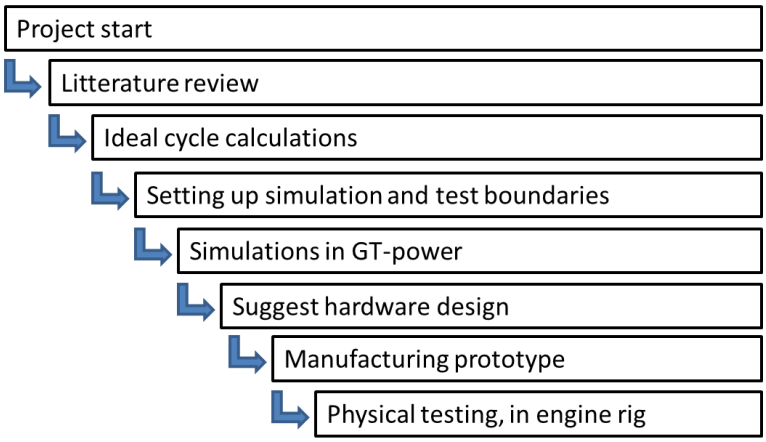

Figure 10- Method overview

Physical tests were performed on the VEP4 MP M1 engine, in order to evaluate fuel efficiency. The modified engine components were manufactured and installed in the VEP4 MP M1 engine which then was tested in the engine rig to evaluate the simulation results. Each step of the method is discussed further in the corresponding chapter. Low load and low engine speeds are prioritized during both simulations and testing, because this is where LIVC would be most beneficial and also where the engine generally operates during regular driving.

3.1 Simulation in GT-Power

The simulation software that has been used for this thesis is GT-power. This software solves one dimensional Navier-Stokes equations, i.e. conservation of continuity, energy and momentum. GT-power models are built up by a number of flow elements such as pipes and flow splits. These are represented by one or several control volumes. Scalar variables such as pressure, temperature, density, internal energy and enthalpy are calculated at the center node of each control volume while vector variables such as flow velocity and mass flux are calculated at the faces (inlet and outlet) of each control volume. The dissipation of kinetic energy and the transformation of kinetic energy into thermal heat are solved by using models for wall friction and temperature. The properties of different fluid species are determined by

its equations of state, i.e. equations for liquid and vapor states. Flow restrictions such as valve flows are modeled using forward and reverse discharge coefficients.

The GT-power simulations were used to evaluate the effects of implementing LIVC. In order to get baseline data to use as a reference, a pre-existing engine model of the VEP4 MP was used; official data for this engine can be found in section *3.3.1 Test rig and engine specifications*. Part load was enabled by implementing a varying orifice diameter as a throttle and wastegate control. The load was then controlled by setting target value for BMEP which adjusted both throttle angle and wastegate opening for a fixed engine speed.

The model uses a combustion model, called FKFS, developed at Stuttgart University. This combustion model calculates the burn rate and aims at having the 50% burnt point at 8 CAD aTDCf. But it also controls knock by retarding the 50% burnt point which requires a value for how sensitive the specific engine is for knock dependent on engine speed. The data used for this comes from previous testing of the baseline engine and is kept constant through all simulations. The combustion model also regulates air fuel ratio in order to prevent knock. Since the model has been calibrated against the VEP4 MP engine it is assumed to be accurate for the baseline engine.

In GT-power there are parameters for the piston/bore area and head/bore area ratio. GT-power does not vary these parameters automatically when the compression ratio is changed. This would affect the cooling losses which imposes a source of error when only the compression ratio is increased. This is because the surface to volume ratio does not change in the same way as it would in reality.

Main convergence requirements are set for engine torque, turbine speed and wastegate diameter. The type of convergence requirement and tolerance for the main controllers can be seen in *table 2*. The maximum number of cycles allowed was set to 400 and the minimum to 40 cycles.

Table 2 - Convergence criteria

Part	**Turbine Speed**	**Torque**	**Wastegate diameter**
Type of criteria	Cycle to cycle	Cycle to cycle	Cycle to cycle
Type of tolerance	Fractional	Percentage	Absolute
Tolerance	0.01	0.5	0.2
Number of cycles	5	5	4

Simulated engine speeds and loads where chosen according to *table 3* which resulted in 42 operating points as all loads are simulated at each engine speed. These operating points were chosen so that the resolution is higher at low engine speeds and low loads where the effects of LIVC wanted to be studied more thoroughly. The number of operating points chosen vastly increase the total simulation time as both CR, duration and lift is varied which is why the number of operating points had to be limited since they increase simulation time exponentially. The limited number of operating points can cause information to be missed due

to the limited resolution. However, the resolution is assumed to be adequate in order to detect the trends of varying IVC.

Table 3 - operating points used in simulations and testing

Engine Speed	**1000**	**1500**	**2100**	**3000**	**4200**	**5500**	
Target BMEP [Bar]	2	4	6	8	12	16	23

All simulations with LIVC were done using a turbocharger from the VEP4 LP (low performance) engine. This turbocharger is smaller and better matched with the lower mass flows and maximum torque of the LIVC-engine. The friction model remains the same throughout all simulations.

3.1.1 Intake camshaft simulations

In GT-power a valve motion can be entered as instantaneous lift, s, as a function of CAD. Lift curves needed to be generated that had independently controllable lift and duration. One way of doing this would be to scale the original lift curve to a certain lift and duration. However, since this would also scale the ramps of the lift curve this would result in a camshaft that might not be useable in the physical testing phase. Instead a harmonic lift curve was generated according to equation (3.1).

$$s(\theta) = \frac{L}{2}\left(1 - cos\left(\pi \frac{\theta}{dur}\right)\right) \quad where \;\; 0° \leq \theta \leq 180° \; CAD \quad (3.1)$$

The original lift curve for the VEP4 MP engine has a duration of 227 CAD and maximum lift of 8.57 mm. This curve can be seen in *figure 11*. If compared to the harmonic lift curve, dashed line, using the same values for lift and duration it shows a clearly visible difference, especially at the start and end of the valve lift. Because of the direct acting camshaft, the initial ramp with constant acceleration is needed. This is why equation (3.1) was combined with the ramps of the original lift curve, using the same duration and lift. This results in the modified harmonic lift curve seen in *figure 11*.

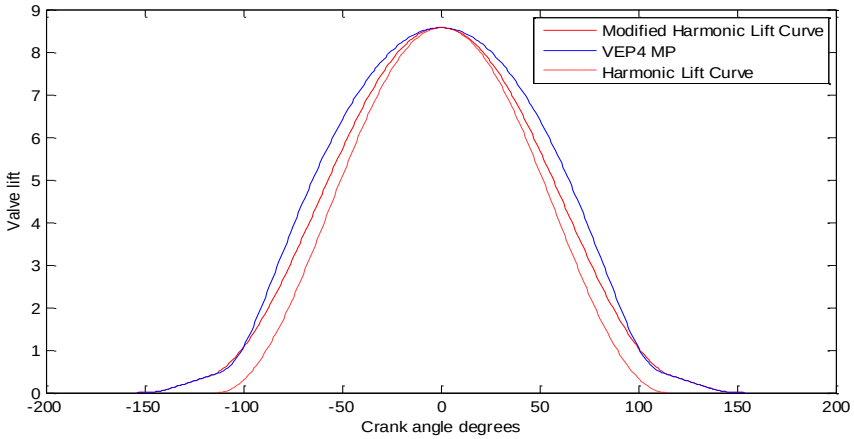

Figure 11– Creating the valve lift curves which are used in the simulations

Using this method, lift curves with different duration and lift could be generated. The duration and valve lift simulated in GT power is seen in *table 4*. Note that all durations and compression ratios were combined with all the lifts in the table. These intervals where chosen because manufacturing restrictions of about 260 CAD duration on the camshaft were identified if 10 mm maximum lift was to be achieved and the original castings were going to be used. Since the original cylinder head was going to be used, it created a restriction in maximum possible lift of about 10 mm. An interval around these restrictions were therefore simulated.

Table 4- Camshaft and piston geometry sweep

Max Lift	7	8.5	10
Duration	240	260	280
CR	12:1	13:1	14:1

The VVT was set constant for both intake and exhaust during all simulations. It was set to have IVO at TDC and EVC at 10 CAD aTDC. One advantage of choosing IVO at TDC and not use the VVT is that the duration of the camshaft can easily be translated into IVC, i.e. a duration of 280 CAD has IVC at 280 CAD aTDCnf. This gives IVC at 60, 80 and 100 CAD aBDC for the different camshafts as can be seen in *figure 12*. Even though a constant IVO gives a flow restriction around TDC, it provides a reference to be able to compare the results of different IVC.

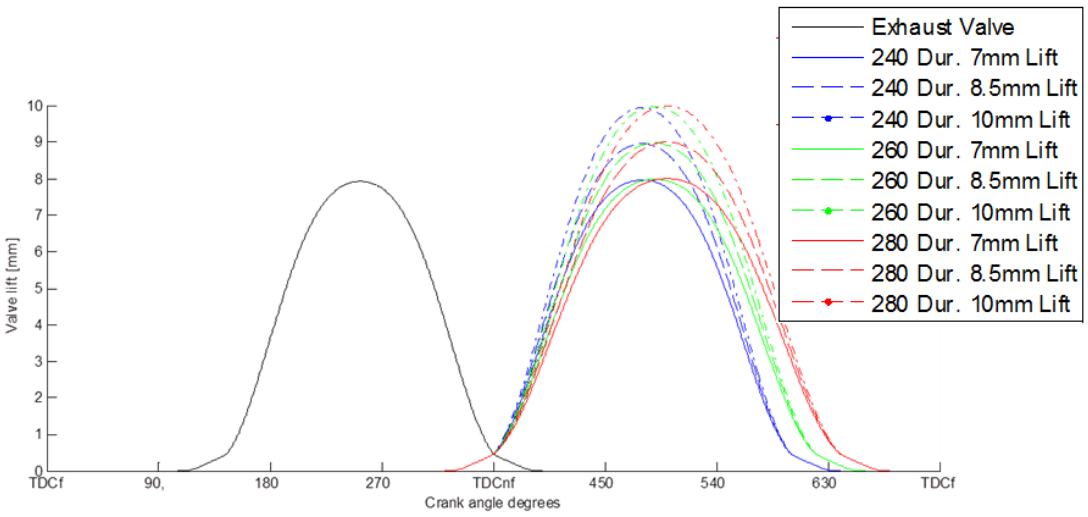

Figure 12 – Simulated intake valve lift profiles

3.1.2 Compression ratio

Since LIVC reduces the effective CR as air is pushed back out from the cylinders to the intake, the geometric CR must be increased to obtain high efficiency. GT-power simulations were therefore performed for CR 12:1, 13:1 and 14:1. This showed that geometric CR above 13:1 is preferred and further simulations were therefore performed for compression ratios between 13:1 and 15:1 with a step size of 0.25. 15:1 was chosen as maximum since it is

experimentally shown [17] to be a limit in order to achieve maximum total efficiency at part load. The input parameter used in order to change CR in GT-power is only a constant value. Geometry changes of the combustion chamber due to increased CR were not considered in the simulations and consequently, the combustion chamber geometry parameters were kept at the settings of the baseline engine. This is also true for surface/volume ratio which is kept at the baseline value even though it increases as CR is increased. The simulations were only performed for the camshaft geometry selected for the LIVC-engine. This has 280 CAD duration and 6.8 mm lift and the simulations were performed for the operating points specified in *table 3*.

3.1.3 Estimating fuel consumption using BSFC-maps

By observing the load map and BSFC values from simulations of different camshafts it is hard to assess the effect the changes has on for instance a real life driving situation. In order to get values that are easily comparable and understandable it was desired to estimate the fuel consumption for the different engine setups. Therefore a method for calculating fuel consumption from the already existing BSFC-maps was designed. In order to get relevant operating points, data from the Artemis driving cycle was used. The Artemis driving cycle was derived from data collected by vehicles in real world traffic in order to accurately evaluate pollutant emissions. Data used for the Artemis driving cycle is presented in *figure 13*. Note that this method was used to get a relative comparison between different engine setups, not necessarily an absolute fuel consumption value representative of the actual vehicle.

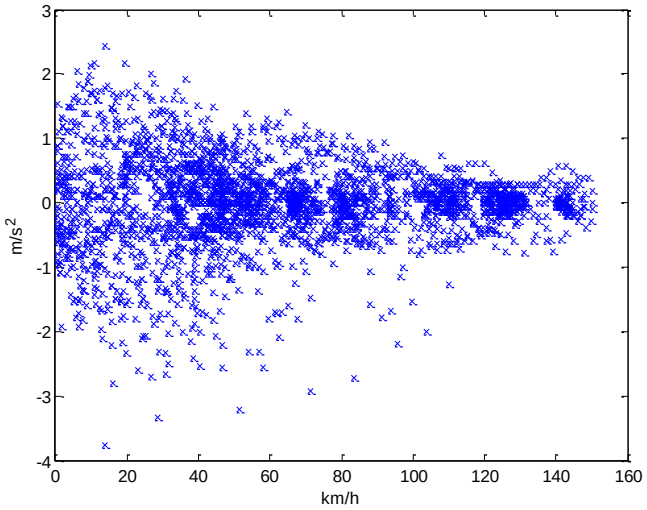

Figure 13 - Artemis driving cycle data

Instead of using all data points to estimate fuel consumption, four vehicle speeds were chosen to represent the data in order for calculations to be more time efficient. The vehicle speeds chosen were 40, 80, 120 and 160 km/h, and the average accelerations was calculated at an interval of 40 km/h at each of those speeds. The fuel consumption estimation is then done using an operating point of constant speed and one operating point of constant acceleration at each of the chosen speeds. The reason for having one operating point of constant acceleration

and one for constant speed is to more accurately describe real-world driving situation and therefore real-world fuel consumption. The frequency of the different vehicle speeds, 40, 80, 120 and 160 km/h, are calculated as well as the average acceleration and the data is presented in *table 5*.

Table 5 - Artemis driving cycle data simplified

Vehicle speed [km/h]	Frequency	Average acceleration [m/s²]
40	0.4235	0.5516
80	0.2685	0.3627
120	0.2581	0.1956
160	0.0499	0

At 56.51% of the points the acceleration is negative, as the clutch may be used during deceleration the operating point of the engine is hard to predict. For the engine operating point it is instead assumed that constant speed is used 56.51% of the time while acceleration is required 43.49% of the time. Engine breaking is disregarded. In order to calculate fuel consumption, vehicle data from a Volvo S60 was used, according to *table 6* and *table 7*.

Table 6 - Vehicle data used for fuel consumption estimation

Vehicle data Volvo S60		
Vehicle mass	m_v	1600 kg
Drag coefficient	C_d	0.28
Frontal area	A_v	2.27
Displaced volume	V_d	1.969 l
Wheel radius	r_w	0.3262 m
Coefficient of rolling resistance	C_r	0.012
Transmission efficiency	η_{trans}	0.9

Table 7 - Gear ratio used for fuel consumption estimation

Gear Ratios						
1	2	3	4	5	6	Final
3.385	1.905	1.194	0.838	0.652	0.540	3.77

The power demand depends on vehicle speed, v, and the acceleration is then calculated by using equations (3.2)-(3.4).

$$P_{acc} = m_v \cdot v \cdot a \qquad (3.2)$$

$$P_b = \frac{(2.73 \cdot C_r \cdot m_v + 0.0126 \cdot C_d \cdot A_v \cdot v^2)v + P_{acc}}{\eta_{trans}} \qquad (3.3)$$

$$BMEP = 2 \cdot \frac{P_b}{\omega_E \cdot \frac{V_d}{2 \cdot \pi}} \qquad (3.4)$$

Engine speed, ω_E, is calculated using the vehicle speed, wheel radius and total gear ratio. The gearing of the vehicle is then used to set a number of load points applicable to each speed. The lowest gear ratio possible is used for each operating point. Note that this requires a downshift for accelerating. The data for each operating point is seen in *table 8*.

Table 8 - Operating point data for fuel consumption estimation

Vehicle speed [km/h]	**P_b, constant speed [kW**	**P_b, accelerating**	**Gear Constant speed/Acc.**	**RPM, Constant speed**	**BMEP, Constant speed**	**RPM, Accelerating**	**BMEP, Accelerating**
40	2.9	13.0	4/3	1100	2.1	1464	5.889
80	9.2	20.2	5/4	1324	4.31	1599	9.047
120	22.4	32.7	6/6	1987	6.825	1987	10.45
160	45.8	45.8	6/6	2649	10.46	2649	10.46

The fuel mass flow is then calculated using equation (3.5). Where the frequency, t_{fr}, of each vehicle speed is multiplied with the BSFC values and the power demand of each operating point.

$$\dot{m}_{fuel} = BSFC \cdot P_b \cdot t_{fr} \qquad (3.5)$$

A consumption value in liters/10km for each engine setup is then calculated according to equation (3.6). This gives results that are easily compared to another rather than the BSFC-map.

$$FuelCons = \frac{\dot{m}_{fuel}}{\rho_{fuel} \cdot v} \qquad (3.6)$$

3.2 Hardware design

This chapter explains the methodology for the hardware design in order to implement LIVC. The new intake valve duration is achieved through changes of the intake camshaft and the geometric compression ratio is increased through a new piston design.

3.2.1 Camshaft design

The results from the GT-power simulations were used as recommendations during the component design. The increased duration was shown to have a larger effect on fuel efficiency than the increased maximum lift. Therefore the camshaft used in physical testing was designed to have a duration of 280 CAD and the maximum lift possible, to be able to use the original castings, was then 6.8 mm. The final lift curve is shown in *figure 14*. The final part of designing the camshaft was done by an engineer at VCC in order to make sure that the

valve accelerations and spring forces are kept within tolerances and to provide accurate manufacturing information and drawings.

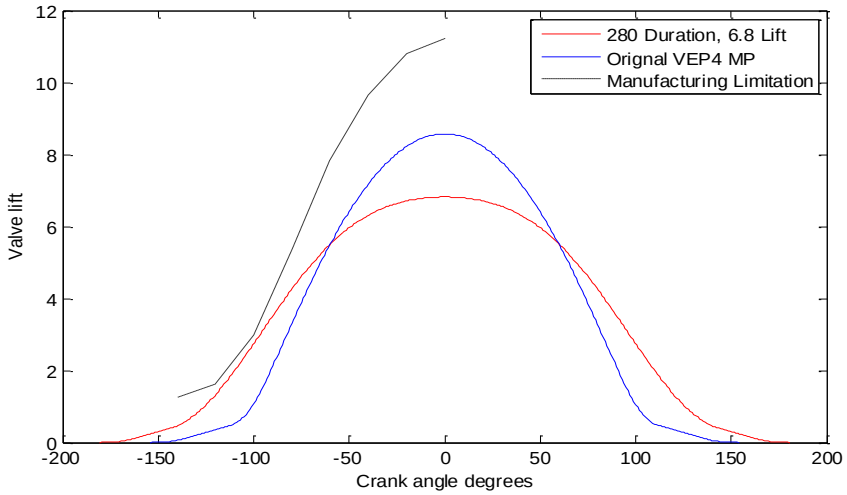

Figure 14 - LIVC camshaft final design

The new lift curve still shares the same ramps as the original one but the remainder of the lift curve is slightly different from the ones that were previously simulated. Therefore the equation describing the valve lift had to be modified. The new equation used to create the lift curve is presented in equation (3.7).

$$s(\theta) = \frac{L}{2}\left(1 - cos\left(\pi\frac{\theta}{dur}\right) - \frac{1}{2}\cos\left(\frac{2\pi\theta}{dur}\right)\right) \qquad 20° \leq \theta \leq 180° \, CAD \qquad (3.7)$$

The VVT range had to be decided prior to manufacturing since these limits are set by the geometry of the camshafts and had to be included in the drawings. Since there was not enough information to base a decision for the range at this point in the project, it was decided to set the mid-point of the VVT-range so that it corresponds to the simulated IVO. This means that it is possible to phase IV VVT ±25 CAD from the GT-power reference values. *Figure 15* displays the original and modified intake camshafts. The top of the camshafts are grinded beyond the maximum grinding depth tolerance which is assumed not to be an issue since the engine is only used for a short testing period.

Figure 15 – LIVC & original intake camshaft

3.2.2 Hardware design, Pistons

Based on the simulation results it was decided that the modified engine should have a geometric CR of 14:1. The baseline pistons were therefore modified to comply with this requirement. Since the increased compression ratio may cause increased cooling losses, the piston was designed to be flat at the top in order to minimize the surface to volume ratio. Also because of the decreased valve lift close to TDC the valve pockets in the original piston was unnecessarily deep for the new intake camshaft. In order to slightly reduce the surface to volume ratio and to achieve 14:1 in CR these pockets were raised by 1.3 mm. The old and new piston is seen in *figure 16*. The pistons were then CNC-milled out of forgings that were close to final shape.

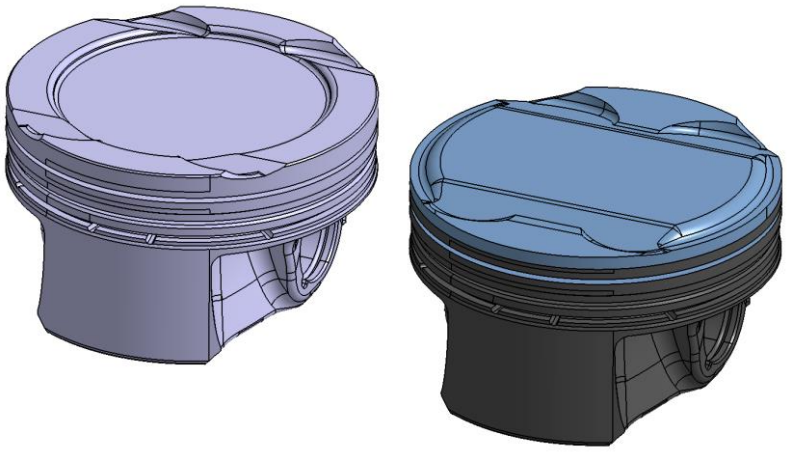

Figure 16 - Piston CR 10.8:1 (left) and piston CR 14:1 (right)

3.2.3 Simulation with complete hardware design

Before manufacturing of the new engine components, simulations were done in GT-power using the complete modified hardware design. The VVT has so far been set at constant values and in order to bring it to a further developed state, closer to the baseline engine, different VVT-settings were simulated. This was also done since it will decrease the time for optimizing and calibrating the engine during the engine tests. The VVT range which was swept in the simulations is seen in *figure 17*. The operating points are the same as in previous simulations and can be seen in *table 3*. The intake camshaft has 280 CAD duration with a maximum lift of 6.8 mm and the CR used is 14:1.

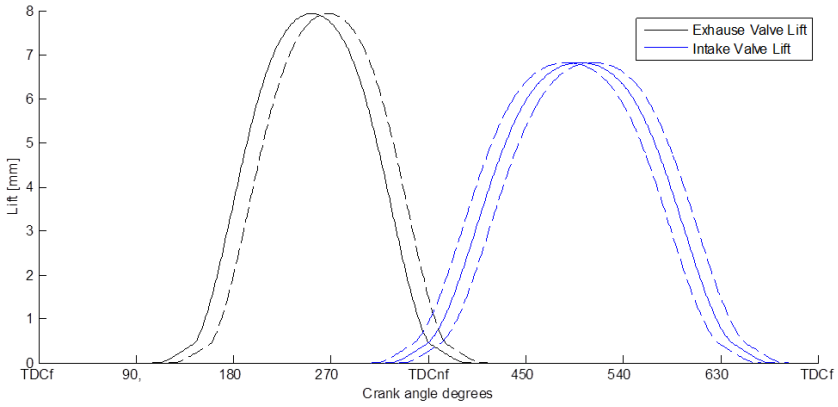

Figure 17 - VVT optimization range

EVC and IVC were varied according to *table 9*. The range of possible IVCs is the same as that available during engine testing. Note that IVO and IVC for this report is defined as the point where the ramps end and start which is further explained in chapter *2.4.1 Valvetrain mechanics and geometry*.

Table 9- VVT simulated

EVC CAD aTDCnf	0	10	20	30	
IVC CAD aBDC	75	90	100	110	125

3.3 Physical testing

This chapter explains how the engine testing was performed and what hardware and software that were used for measuring and calibration.

3.3.1Engine rig and test equipment

The engine used in the tests and simulations is the VEP4 MP M1, developed and manufactured by VCC. VEP4 MP stands for Volvo engine petrol medium performance while M1 says that it is a prototype and not the production engine. The engine has maximum power of 180 kW at 5500 RPM and a maximum engine speed of 6000 RPM. The bore is 82 mm and the stroke is 93.2 mm and the total displacement volume is 1.969 liter with a CR of 10.8:1. The engine produces 350 Nm from 1500 – 4500 RPM, and the official specifications of the engine can be seen in *Appendix A*. The engine installed in the test rig is seen in *figure 18*.

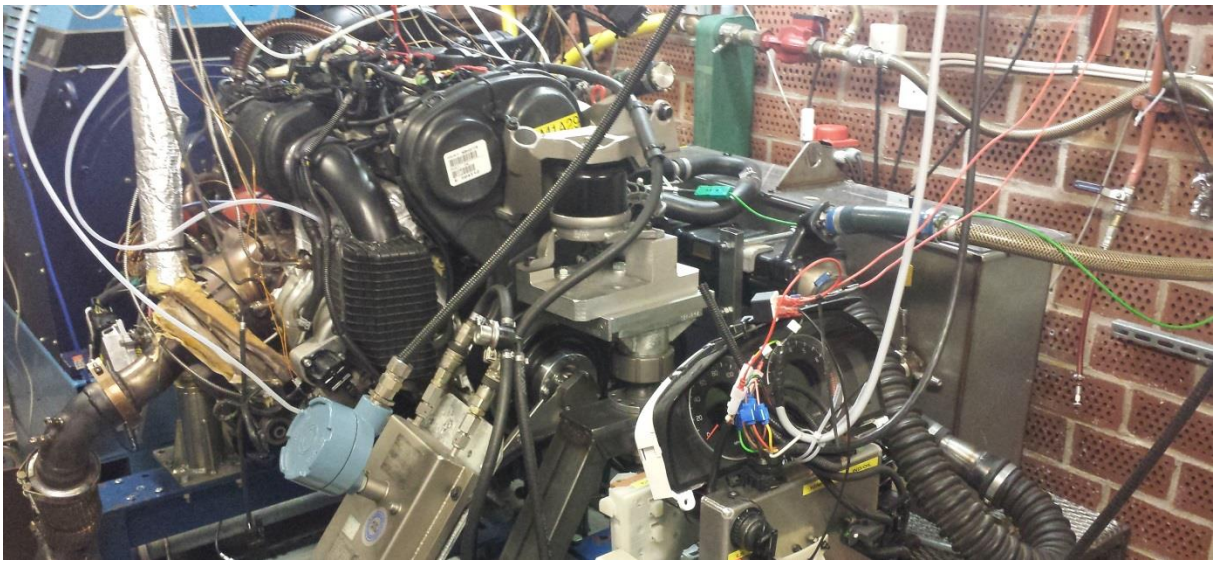

Figure 18 – Engine installed in test rig

The dynamometer in the test rig used during physical testing controls the engine speed and measures the torque the engine produces. The load is controlled by demanding torque from the engine. The ECU then controls the throttle position, ignition timing, valve timing, wastegate, etc. electronically. The test rig controls the engine speed and applies a resistive torque. There are also three computers to monitor the engine's state and to calibrate the ECU. The engine coolant temperature is controlled by a PID controller which regulates the external coolant mass flow and is set to maintain the temperature at 90℃. The charge air cooler is water cooled with recirculating water while the room temperature was dependent on ambient conditions and how long the engine had been running. Because of that the, charge air cooler cools the air to roughly the same temperature independent of room temperature. The room temperature is assumed to mostly affect the efficiency of the turbocharger.

In addition to all the sensors for the ECU there is extra measuring equipment installed in the test rig in order to further analyze the engine state. There are pressure sensors giving instantaneous pressure measurements in each cylinder, which are used to create pressure traces of the combustion cycles. These signals are also used to calculate IMEP and PMEP. The cylinder pressure sensors consist of piezoelectric pressure transducers using a pressure sensitive crystal that generate an electric current as they are compressed. An amplifier then generates an output voltage that is proportional to the pressure which in turn is transferred to a computer that displays, for instance, real time p-V diagrams. The software used is called AVL Indicom v1.5b, and the graphs' main purpose is to monitor the level of knock during calibration.

There are also extra pressure sensors in the exhaust manifold after the turbocharger. Pressure is also measured before and after the compressor of the turbo as well as the ambient pressure. These sensors together with data from the air mass flow sensor could then be used to estimate the operating point of the compressor. Temperature is measured using external thermocouples on the exhaust manifold, between the turbo and catalytic converter, compressor inlet, compressor outlet, intake plenum and runner inlets. The reason for having both intake plenum and runner inlet thermocouples is that the temperature increase from pushing the cylinder

charge back to the intake manifold, is easier to see in the runner. The signals from the previously mentioned measuring devices together with signals from the ECU are transferred via CAN-bus to a computer which uses the software INCA v7.1.3 by ETAS. INCA is used for both reading information from the ECU as well as programming it. The ECU is the same one that is used in Volvos test rigs using software and data that is representative for production values.

Further equipment for measuring emissions as well as a fuel mass flow meter is used. These are sampled on a different computer which operates on a separate system from the previous mentioned. The fuel flow meter measures the fuel flow, $\dot{m}_f$ [g/s]. This can then be used to calculate the BSFC according to equation (3.8). The software used for monitoring the fuel flow and emissions is called LabView v9.0.1 SP1 by National Instruments.

$$BSFC = \frac{\dot{m}_f \cdot 3600}{P_b} \qquad (3.8)$$

A separate weight scale was also used as a complement to the flow meter for measuring the fuel flow. This scale fills up a buffer with fuel and measures the weight change over time. This information is then presented as a fuel flow in [g/s]. Once the fuel buffer is empty, it is automatically refilled. Having two systems to measure the fuel flow provides an opportunity to ensure that the values are accurate.

Physical testing was done in order to verify the simulation results. In order to get proper reference data, engine tests were supposed to be performed on a VEP4 MP M1 baseline engine. At the time when testing started, the engine was already installed in the test rig and had previously been used for other research. Unfortunately the baseline engine was too worn which made the results unreliable and the test of the baseline engine was therefore aborted prematurely. Instead, baseline data from Volvo's test rig had to be used for comparison with the results of the LIVC-engine. This generates uncertainty in the results since data are not collected using the same test equipment. Neither is the engine tested according to the same test procedure. The engine tests were performed for the operating points seen in *table 10*. Each operating point was run a number of times to get several measurements in each operating point. The results are presented as an average value of all measurements for each operating point.

Table 10 - Operating points, physical test plan

RPM	**1500**	**2100**	**3000**
	2 BMEP	2 BMEP	2 BMEP
	4 BMEP	4 BMEP	4 BMEP
	6 BMEP	6 BMEP	6 BMEP
	7 BMEP	7 BMEP	8 BMEP
	8 BMEP	8 BMEP	10 BMEP
	9 BMEP	9 BMEP	12 BMEP
	10 BMEP	10 BMEP	Max
	12 BMEP	12 BMEP	
	Max	Max	

For the baseline test, VEP4-MP M1 code and data was used for the ECU which controlled engine operating conditions, such as lambda, VVT, throttle angle and ignition timing. After the baseline test was concluded, the engine was modified with the new camshafts and pistons and then installed back in the rig. *Figure 19* shows the engine being rebuilt with the new pistons.

Figure 19 - Engine rebuild and modification

The LIVC-engine had to be calibrated manually in order for the engine to operate efficiently. There are many parameters that can be adjusted but for each operating point, mainly four parameters were controlled. These were ignition timing, IV-VVT, EV-VVT and throttle angle. Ignition timing was controlled in order to get the 50% burnt point around 7-8 CAD aTDC or as close as possible to MBT-timing when the maximum ignition advance was limited by knock.

VVT was at first set to have EVC at 10 CAD aTDC and IVO at TDC in order to obtain data comparable to the GT-power reference. The VVT settings were then optimized through iterations in order to minimize BSFC. At the start of each test session measurements were also taken on a reference point in order to make sure that the measuring equipment showed roughly the same values and that engine was operating properly.

For both the baseline engine and the LIVC-engine, tests were done with a lambda target of 1.00, i.e. stoichiometric conditions unless the ECU increased fuel/air ratio to prevent knock or damage to the aftertreatment system. The lambda value is measured by three different O2-sensors connected to the ECU. A lambda value was also calculated by LabView based on the engine out emissions.

4. Results

This chapter presents the results from the simulations of various IVC, intake valve lifts as well as compression ratios. It also shows the difference between the simulation results for the LIVC-engine using the final hardware design and the baseline engine. Experimental results from the engine tests of the LIVC-engine are then shown and compared with data from VCC's baseline tests at the end of this chapter.

4.1 Simulation results

The simulation results are divided into three chapters were results from simulating various IVC, lifts and compression ratios are presented individually.

4.1.1 Effects found from increasing IV duration

Since the aim of the project was to increase fuel efficiency the BSFC is of main concern. *Figure 20* shows the BSFC maps for the first simulation run for different compression ratios and different IV duration and lift. Note that values between the simulated operating points are interpolated.

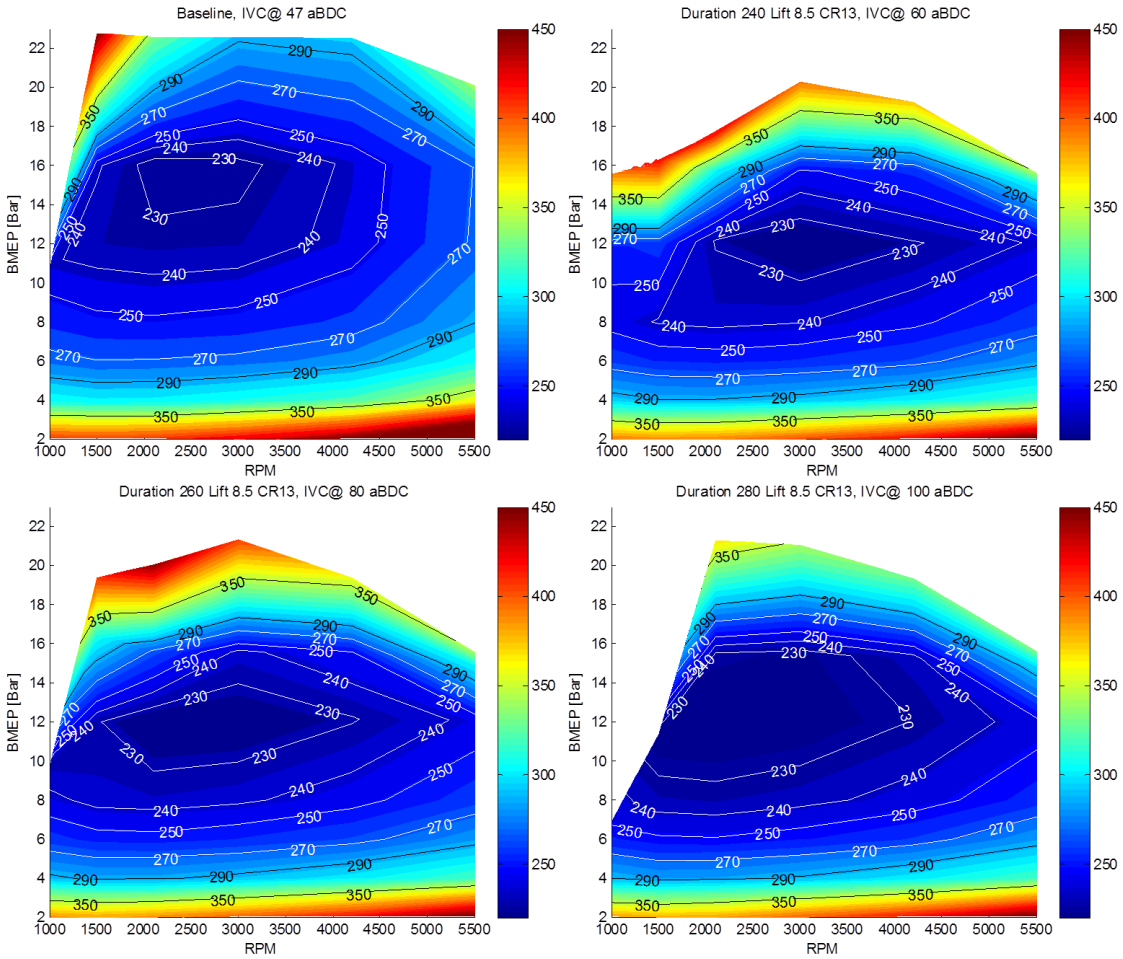

Figure 20 – BSFC, with IVC at 47 (baseline reference), 60, 80 and 100 CAD aBDC

In *figure 20* it is visible that increased duration pushes the area with BSFC below 250 g/kWh towards lower loads. For the baseline engine a BSFC below 250 g/kWh is reachable above 9 bar BMEP while with IVC at 100 CAD aBDC, 250g/kWh is reached around 6.5 bar BMEP and for a wider engine speed range. It is also visible that the area of sub 250 g/kWh increases in size for the longer IV duration. However, at engine speeds below 1500 RPM the maximum torque is heavily reduced with IVC at 100 CAD aBDC.

In *figure 21* the BSFC values for three different engine speeds are presented. In order to compare the influence LIVC has on BSFC, the values were normalized against the BSFC of the baseline engine. This data is also presented in *figure 21*. A BSFC decrease of 7% can be seen at lower loads and engine speeds. As the load increases above a BMEP of 12 bar, the baseline engine's BSFC is lower than for the LIVC-engine. This is due to that the model adapts the ignition to prevent knock.

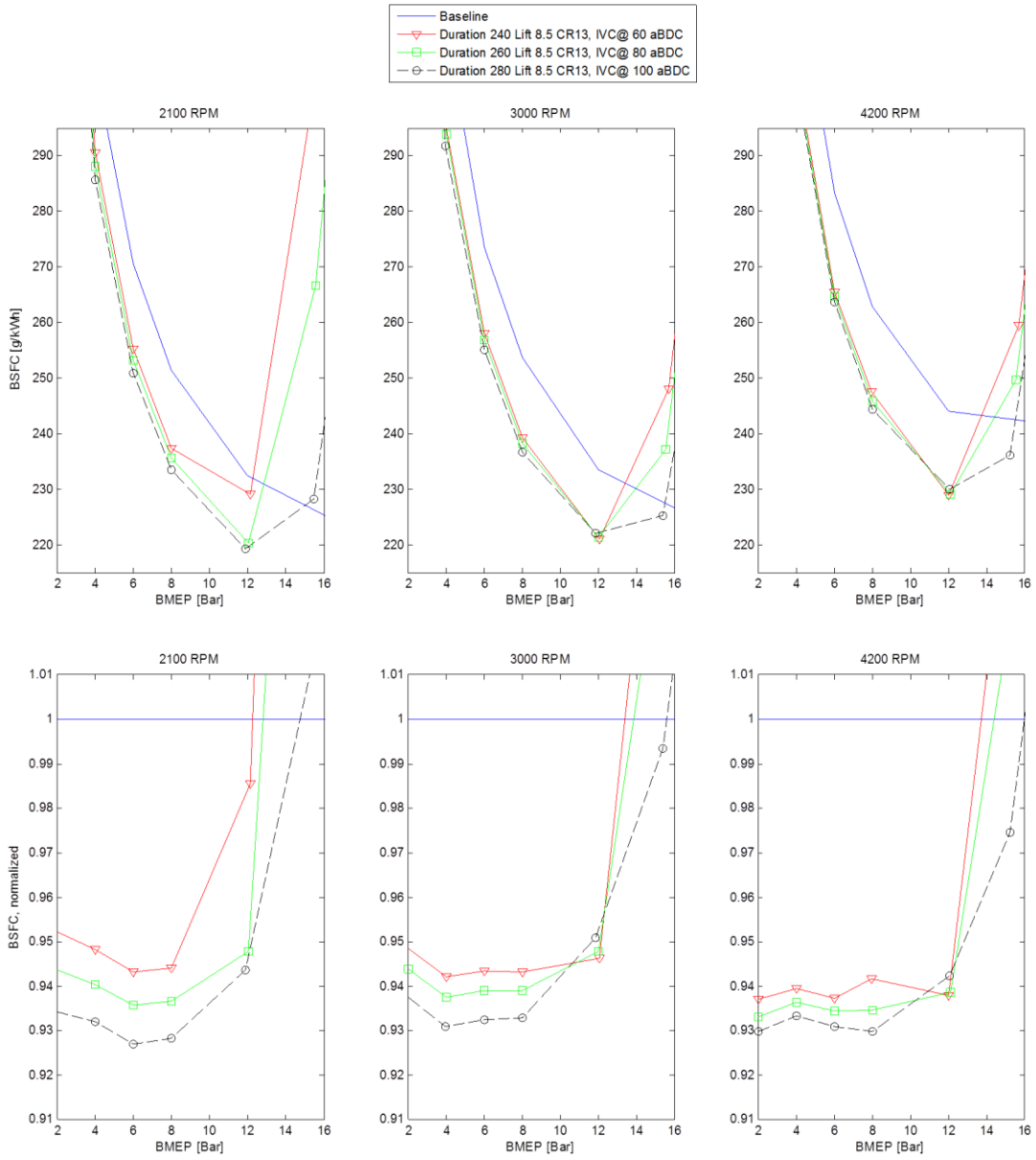

Figure 21 – BSFC depending on IVC

The results suggest that an increased duration within the researched interval improves BSFC below 12 Bar BMEP. At 2100 RPM the LIVC engine reaches 219.3 g/kWh in BSFC at 12 bar BMEP. It is an improvement of 5.6% compared to the baseline engine which reaches 232.4 g/kWh at the same operating point. At loads above 12 bar BMEP the baseline engine's fuel efficiency is higher than for the LIVC. It can be seen that the optimum BSFC point for each RPM moves towards lower loads with LIVC. What all the LIVC setups have in common is that above 12 Bar BMEP the 50% burn point deviates from 8 CAD aTDC, this means that the model adjusts the start of combustion in order to prevent knock and this is why the BSFC improvement is limited above this load point. At low engine speeds a 5% improvement in BSFC is achieved for IVC at 60 CAD aBDC compared to 7% improvement for IVC at 100 CAD aBDC.

The PMEP for different IVC can be seen in *figure 22*. For 2100 RPM the pumping losses has decreased for all loads while for the higher engine speeds, decreased pumping losses can be seen for loads below 8 bar BMEP for the latest IVC.

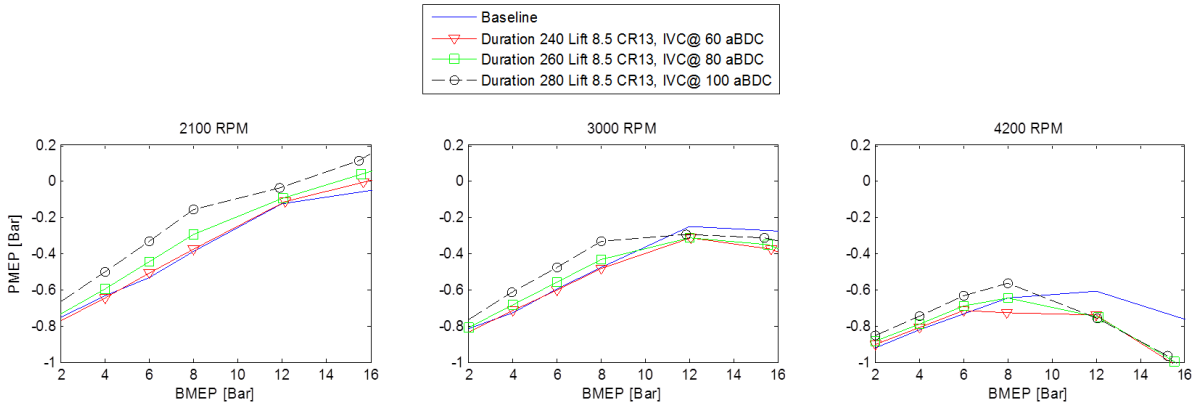

Figure 22 – PMEP depending on IVC

The effects from changing IVC is, as can be seen highly engine speed dependent. If studying the mass flow through the intake valves for two different engine speeds it is clearly visible that for higher engine speeds the ram effect decreases the air mass that is being pushed back into the intake. In *figure 23*, IVC at 100 CAD aBDC can be seen for 2100 RPM and 5500 RPM. This can be a desired effect as it can improve volumetric efficiency and power output but it also increases the effective compression ratio and reduces the effect of LIVC. Higher effective CR results in higher cylinder pressures which increase the knock propensity.

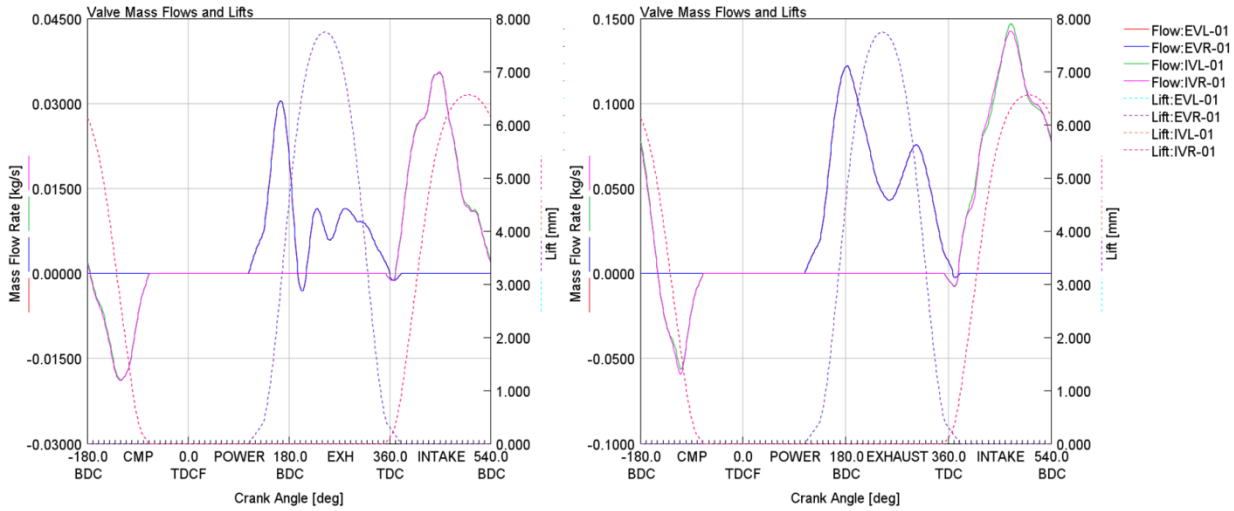

Figure 23 – Mass flow through valves for 2100 rpm and 5500 rpm

The over-expansion is also expected to reduce the exhaust gas pressure and temperature, as can be seen in *figure 24*. The exhaust gas temperature decreases as the ratio between ER and CR increases. Also even though the smaller turbo is expected to generate more back pressure the simulation results points toward a slightly lower exhaust gas pressure with LIVC below 8 bar BMEP.

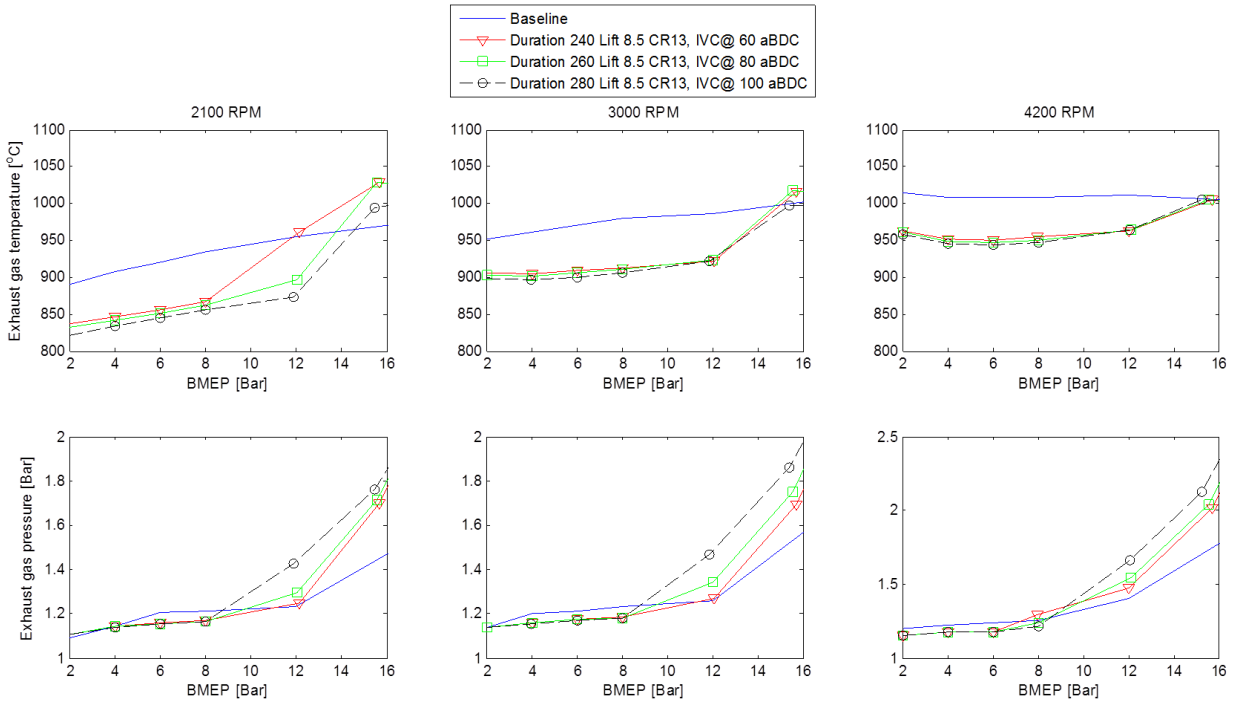

Figure 24 – Exhaust gas pressure and temperature for different IVC

4.1.2 Effects found from altering the valve lift

Altering the valve lift for IVC at 100 CAD aBDC affects BSFC by less than 1 percentage, as can be seen in *figure 25* where BSFC for various lifts are normalized against the BSFC of the baseline engine. At higher engine speeds the difference in BSFC between the simulated valve

lifts is larger. This is due to the increased mass flow which causes the lower valve lift to be more of a restriction than it is for low engine speeds.

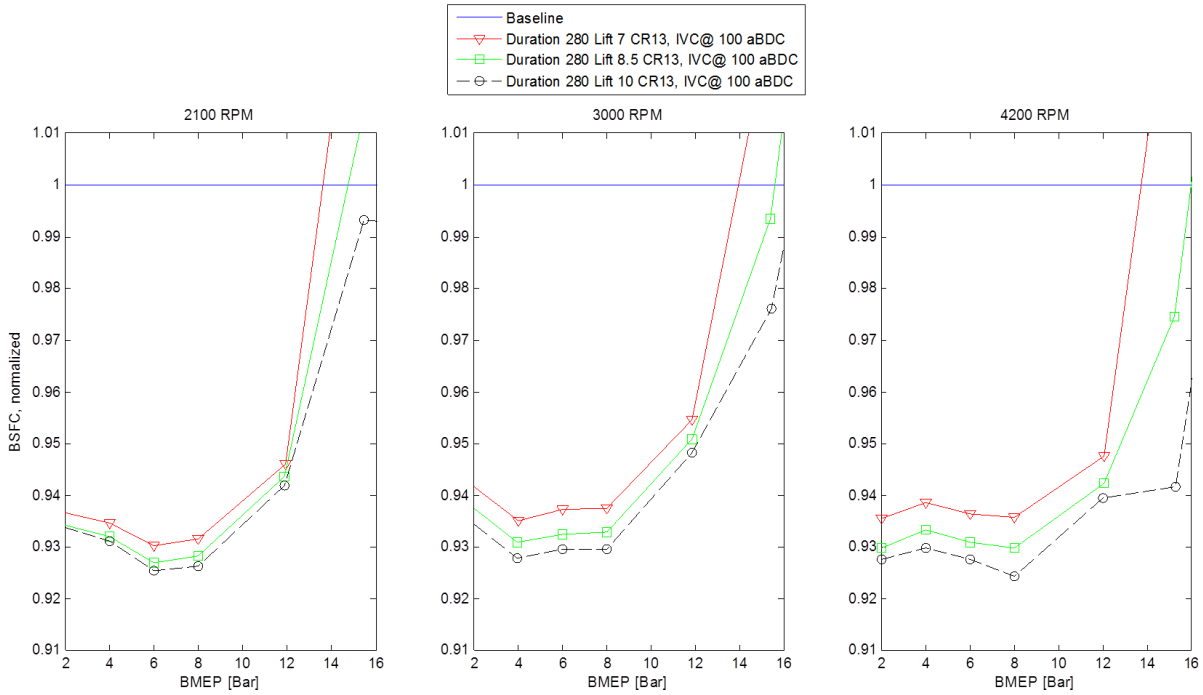

Figure 25 – Normalized BSFC for varying maximum intake valve lift

Another effect found from increasing the lift is that the maximum torque for each engine speed is slightly increased. This effect is also larger at higher engine speeds as the low valve lift again restricts the mass flow across the valves. Increasing the valve lift shows only benefits within the simulated region, if the increased forces within the valvetrain are disregarded.

However, while increasing the lift shows a reduced BSFC of 0.5% to 1%, the increased duration is what improves efficiency the most. Because of this, increasing the duration was prioritized over increasing the lift when designing the new camshaft to fit within the original castings. The final design of the camshaft has 280 CAD duration and 6.8 mm in maximum lift. This was the maximum amount of lift that could fit the casting if 280 CAD duration was to be achieved.

4.1.3 Compression ratio

Figure 26 shows the simulated load maps for an intake camshaft with 280 CAD duration (IVC at 100 CAD aBDC) and 10 mm lift with simulated geometric compression ratios 12:1 and 13:1. From this figure it could be observed that the BSFC values at part load operation decreases with higher compression ratio. It could also be observed that an area of low BSFC, for example the area of 250 g/kWh, is increased in size and present at lower loads. This is due to increased temperatures at the start of combustion caused by higher peak pressures which ultimately increases the thermal efficiency. LIVC causes the effective CR to drop below the geometric CR which allows high geometric CRs to be used without increasing the knock propensity at part load. At higher loads and engine speeds however, high boost pressure in

combination with ram effects of the intake valve flow causes high pressure and temperature at the start of combustion. This increases the knock propensity and the knock model in GT-power then retards the ignition which explains the increase in BSFC observed at higher loads.

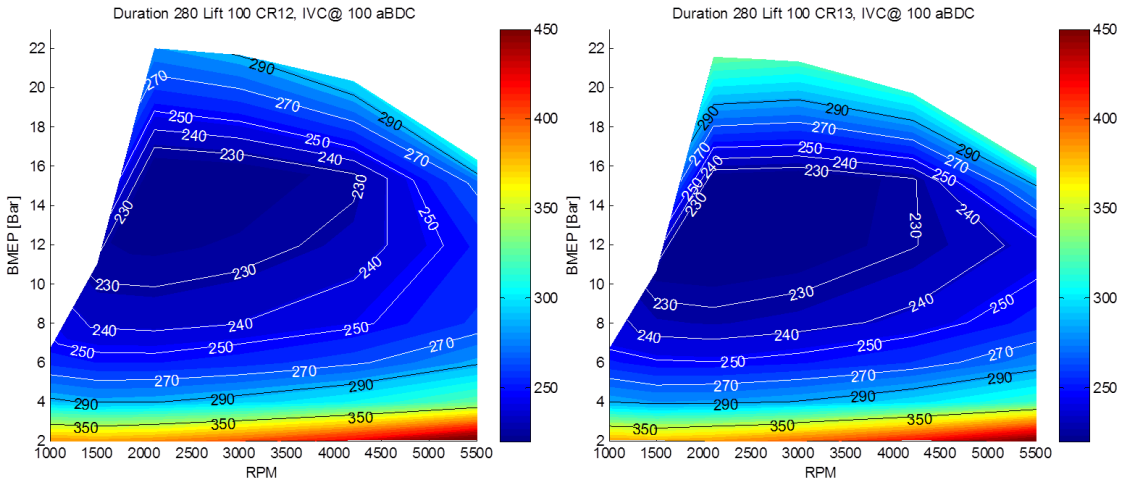

Figure 26 – BSFC map for CR12:1 and CR13:1

Since LIVC has largest effect on BSFC for part load operation it was, based on these observations, decided to aim at a compression ratio above 13:1. Further simulations were therefore performed for compression ratios between 13:1 and 15:1. *Figure 27* shows the results for BSFC for three engine speeds. The BSFC values are normalized with the BSFC values for the baseline engine.

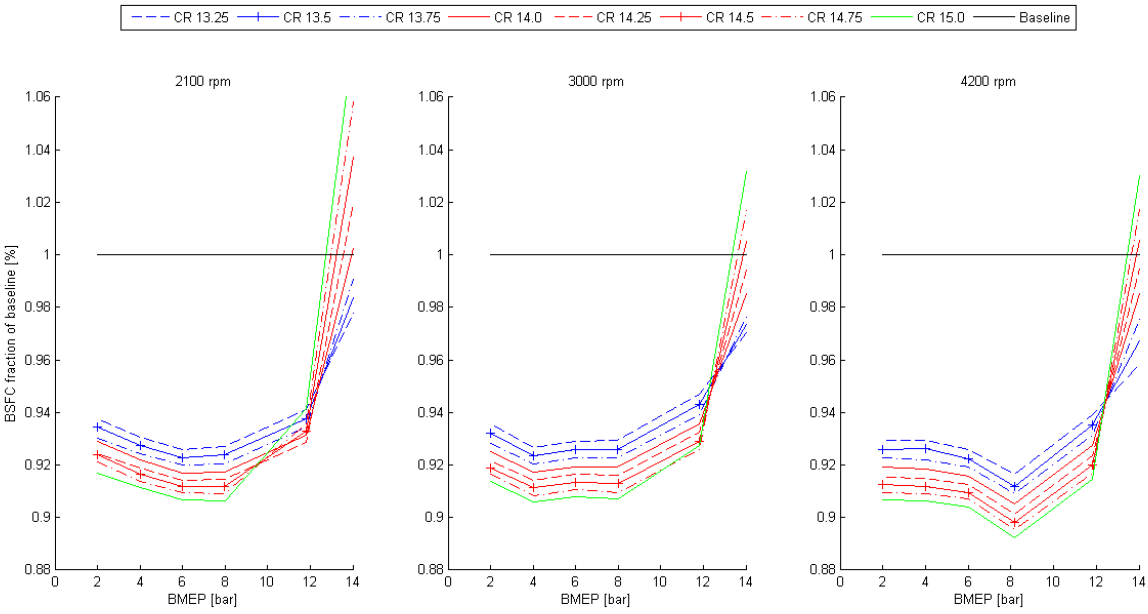

Figure 27 – BSFC normalized with baseline BSFC, for different geometric CR

As can be seen in *figure 27*, BSFC decreases with around 1 percentage for each unit the CR is increased. It could also be observed that BSFC increases rapidly for loads higher than approximately 8 bar for the highest CR. This behavior could be derived from increased knock propensity which causes the combustion model to retard the ignition timing leading to

decreased fuel efficiency. It could also be seen in *figure 28* which shows the CAD where 50% mass fraction of fuel has burnt. This clarifies that a geometric CR as high as 15:1 would make it impossible to reach MBT timing for a large part of the load map since this behavior is consistent for all engine speeds. Since BSFC decreases with approximately one percentage for each CR unit, it was decided to aim for a CR of 14:1. This value was chosen because it is the highest CR that can reach MBT-timing at 12 bar BMEP for engine speeds above 2100 RPM. A geometric CR of 14:1 gives effective CR of 5:1-10:1 (depending on VVT-settings) which gives a ratio ER/CR of 1.4-2.9.

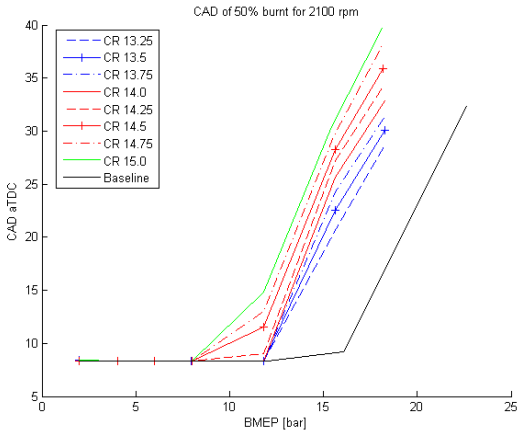

Figure 28 – 50% mass fraction burnt point over BMEP for varying CR

4.1.4 Estimated fuel consumption

Results in fuel consumption estimations can be seen in *figure 29*, where the fuel consumption is normalized against the fuel consumption of the baseline engine. Noticeable is that within the simulated area a trend can be seen that increased duration, increased lift and increased compression ratio decreases the fuel consumption monotonically. Simulations suggest that a decrease of 8% in fuel consumption can be achieved for the longest duration, highest lift and a CR of 14:1.

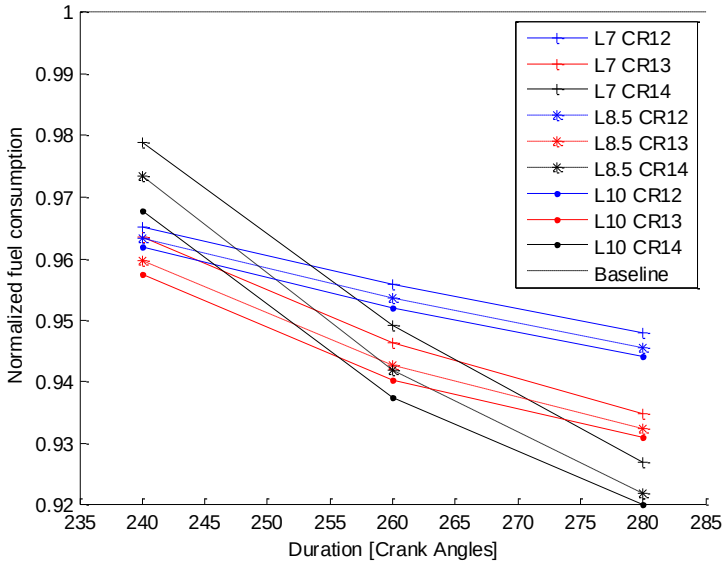

Figure 29 – Normalized estimated fuel consumption over intake valve duration

4.1.5 Comparison of simulation results for baseline engine and modified engine

Based on the findings from the previously described simulations a suggestion of modifications to the baseline engine was developed. The suggested modifications involved switching the intake camshaft to a camshaft with longer duration to enable LIVC, but also to modify the pistons to obtain higher geometric CR. Since LIVC causes lower effective CR, increasing the geometric CR was considered to be necessary in order to obtain as high efficiency improvements as possible. Specifications of the engine modifications are shown in *table 11*.

Table 11 – Engine modifications, LIVC-engine

Engine modifications:	
Intake camshaft duration	280 CAD
Intake valve lift	6.8 mm
IVO @	+/- 25 CAD aTDC (depending on VVT-setting)
IVC @	75-125 CAD aBDC (depending on VVT-setting)
Geometric CR	14:1

A comparison of the simulation results for the baseline reference and the modified engine with LIVC are presented below. These results show the expected outcome with the implementation of LIVC. *Figure 30* shows the BSFC plots for the two engine setups.

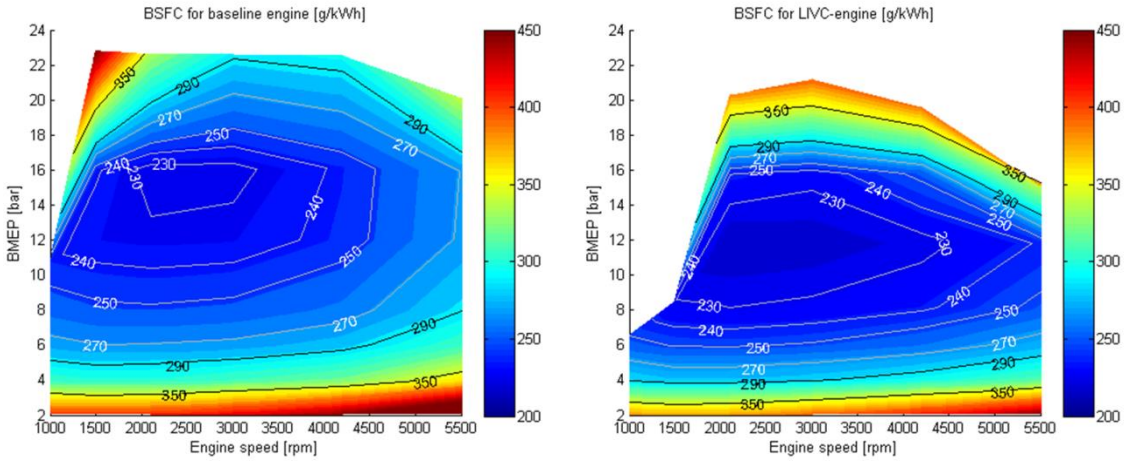

Figure 30 - BSFC comparison for the baseline engine vs. LIVC-engine

As can be seen the maximum torque output from the engine that utilizes LIVC is heavily restricted compared to the baseline engine. However, the reduction in BSFC for part load operation for the modified engine is clearly visible. Notice for example the area of 250 g/kWh which has increased in size and occurs for lower loads compared to the baseline engine. The same trend could be observed over a majority of the load map. Notice also that the minimum BSFC is lower with LIVC, 216.5 g/kWh for LIVC compared to 225.2 g/kWh for the baseline reference. Improvements of 7-8 % with LIVC are obtained for a large part of the load map. A part of the BSFC improvements with LIVC comes from decreased pumping losses. *Figure 31* shows the PMEP comparison for the two engine setups.

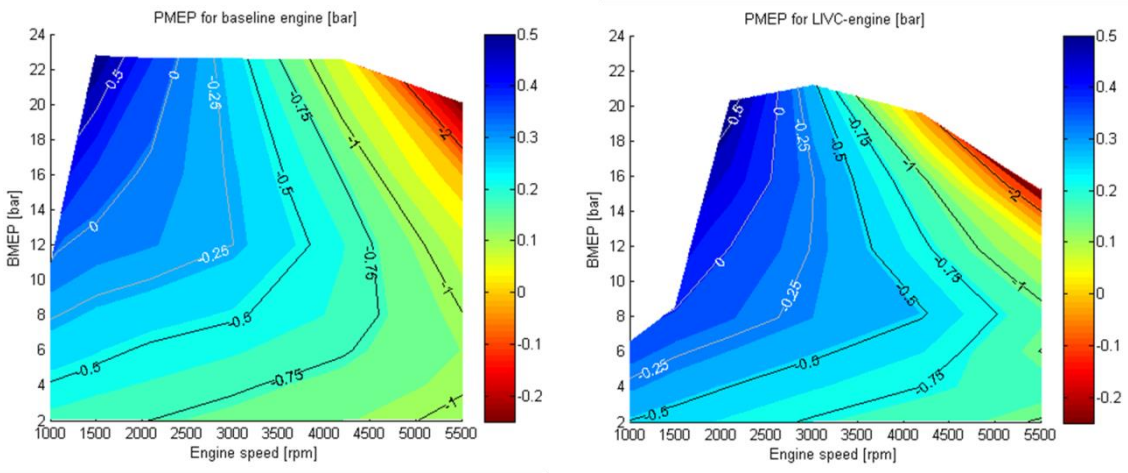

Figure 31 – PMEP comparison for the baseline engine vs. the LIVC-engine

The decreased PMEP for the engine utilizing LIVC is clearly visible. Notice for example how the line of -0.25 bar PMEP occurs for lower loads with LIVC compared to the baseline reference. This is due to the requirement of increased intake pressure to achieve a certain load with LIVC compared to the baseline engine since the effective displacement volume is considerably lower with LIVC. PMEP reductions in a wide range between 12% up to 60% are obtained over a large part of the load map with LIVC. Another expected effect of LIVC is

increased intake temperatures due to the pushed back charge during the compression stroke. This effect is clearly visible in *figure 32* showing increased intake temperatures over the entire load map. This is a negative effect of LIVC since higher intake temperatures increase the knock propensity and decrease the density of the incoming charge.

Also lower EGTs were expected as an effect of the over-expansion since a larger portion of the energy during the expansion stroke is used to produce work on the piston meaning a reduction of heat rejection with the exhausts. *Figure 33* shows the EGT comparison between the modified engine using LIVC and the baseline reference. As can be seen the temperatures are generally lower over the entire load map with LIVC compared to the baseline reference. Notice also the high temperatures for high loads which could set a limit for the maximum torque curve.

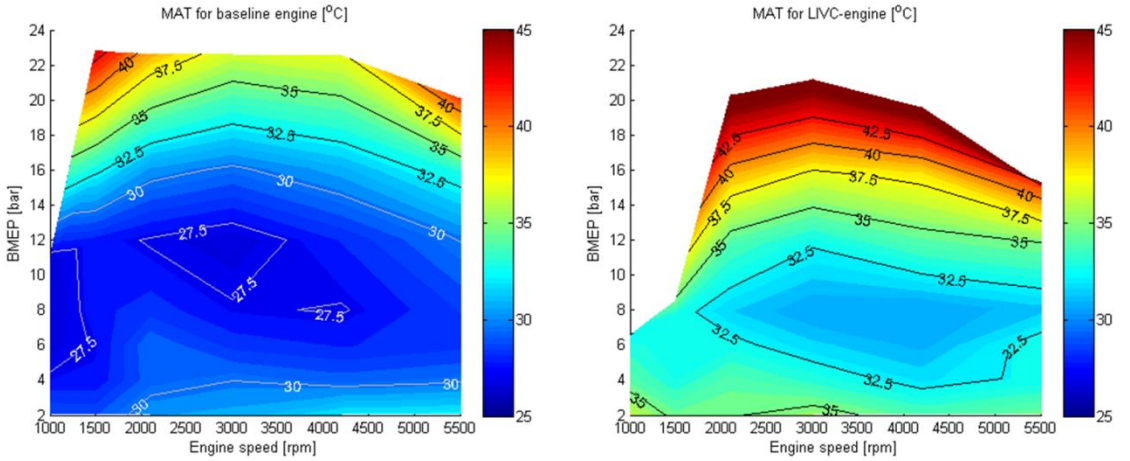

Figure 32 - MAT comparison for the baseline engine vs. LIVC-engine

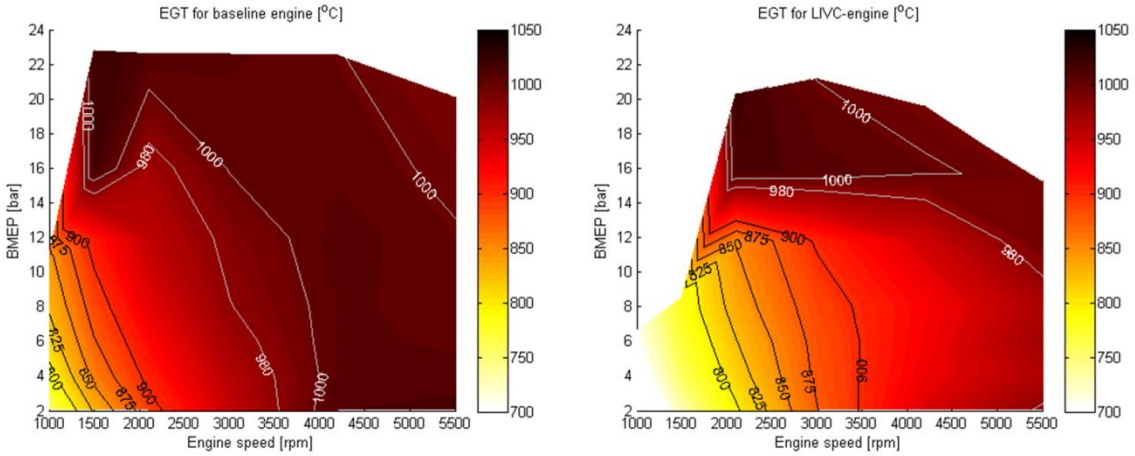

Figure 33 - EGT comparison for the baseline engine vs. LIVC-engine

4.2 Experimental results from engine tests

The physical testing started with the baseline engine, unfortunately it was quickly discovered that there was severe engine damage causing intense knock. This caused the ECU to retard ignition at all operating points above 4 bar BMEP, which in turn resulted in high BSFC. The baseline data therefore comes from a test rig at Volvo, also using the VEP4 MP M1. The emissions before the catalyst were measured during the tests of the LIVC-engine. However, they were not evaluated nor discussed in this project and they are therefore presented in *Appendix B.*

The results for BSFC for both the LIVC-engine and the baseline engine can be seen in *figure 34*. As can be seen the BSFC values are higher than the simulations suggested. The BSFC deviates further from the simulation results as load and engine speed increases.

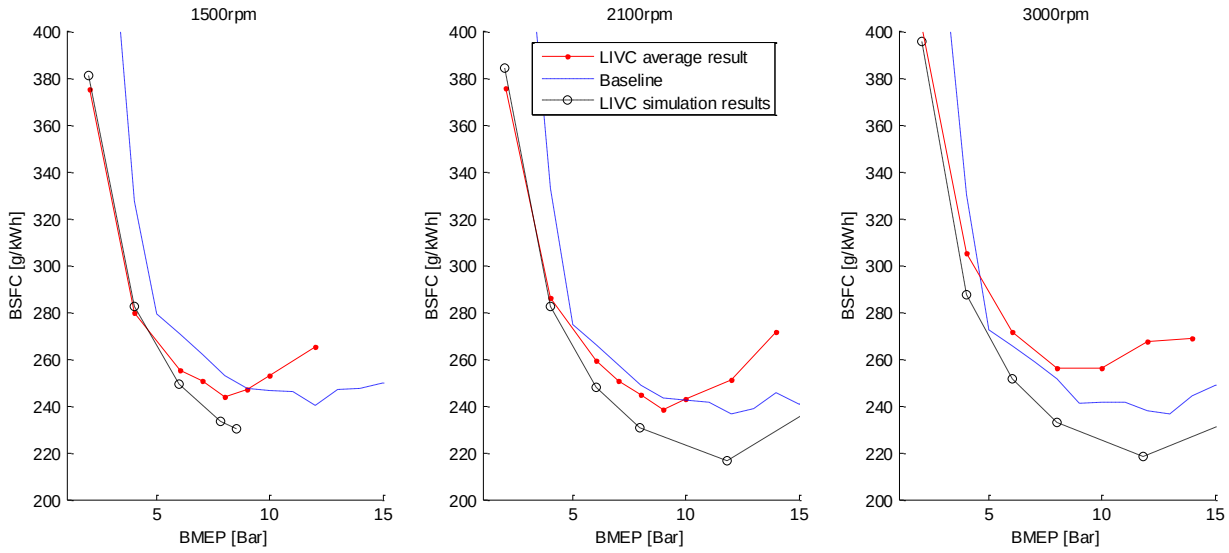

Figure 34 – BSFC values for the LIVC-engine and the baseline engine for 1500, 2100 and 3000 RPM

The lowest BSFC found for the LIVC-engine was 238.6 g/kWh at 2100 RPM 9 bar BMEP. The same operating point for the baseline engine reaches 243.4 g/kWh, an improvement of 2%. Since the baseline test was not performed using the same operating points as the LIVC-engine, the baseline had to be linearly interpolated. *Figure 35* shows the LIVC-engine's BSFC percentage change compared to the baseline BSFC.

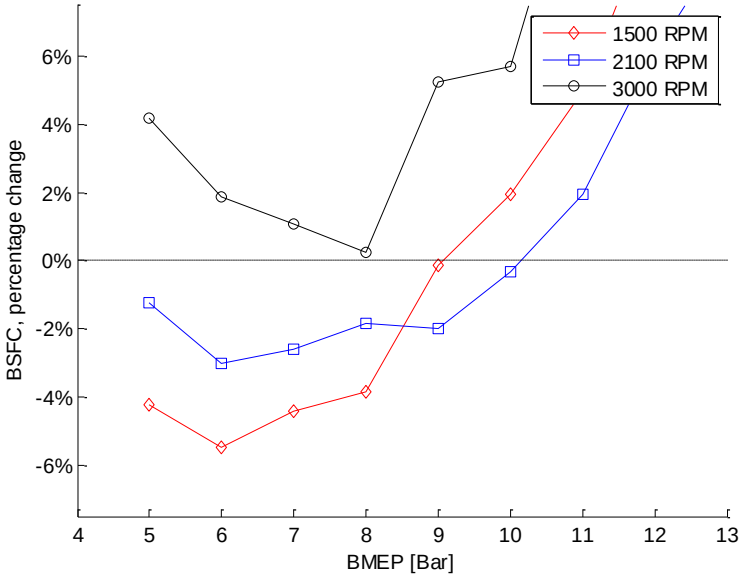

Figure 35 – BSFC percentage change compared to baseline BSFC

As can be seen for 1500 RPM an improvement of 4-6 % can be seen for loads up to 8 bar BMEP and below. For 2100 RPM the improvement is roughly 2 % up to 9 bar BMEP. As for 3000 RPM no improvement can be seen. The expected results according to simulations were about a 7-8% improvement at all engine speeds tested.

The results suggested a major improvement at 2-4 bar BMEP for all engine speeds tested, this is because that operating point was not tested for the baseline engine and because a linear interpolation at such low loads is inaccurate which generates an error. This is why the result is not presented in the graph. Improvements at lower BMEP is therefore assumed to be similar as for the BMEP above because this trend has been noticeable in the simulation results.

At loads above 10 bar BMEP the BSFC is increased for all engine speeds tested and no improvement can be found. The break-off point where the baseline exceeds the LIVC engine in fuel efficiency is found at lower loads than expected. The optimum BSFC point for each engine speed occurs at lower loads than the simulation results suggest. This is because the ignition was limited by engine knock and above 8bar BMEP the 50% mass fraction burnt point does not reach 7-8 CAD aTDC, as can be seen in *figure 36*.

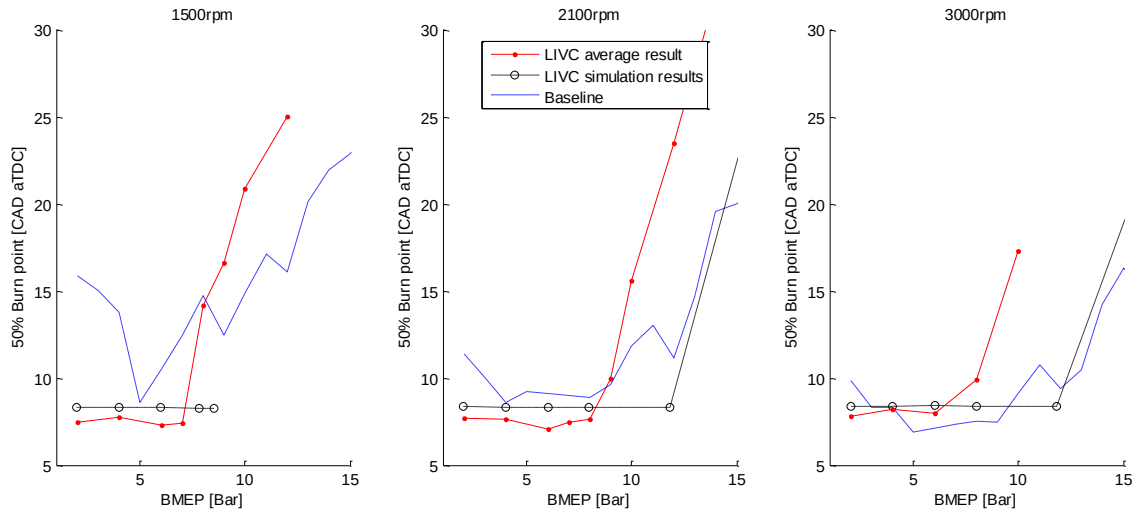

Figure 36 – 50% mass fraction burnt point for the LIVC-engine for 1500, 2100 and 3000 RPM

The measured PMEP can be seen in *figure 37* where it is compared to the PMEP obtained from both the simulations and from the baseline tests from VCC. As can be seen there is a reduction in pumping work for the LIVC-engine at engine speeds between 1500-2100 RPM when it is compared with the baseline results. At 1500 RPM the pumping work reduction is also higher than what the simulations suggested which is also true for low loads at 2100 RPM. At 3000 RPM the pumping losses are a lot higher for the LIVC-engine compared to both the baseline engine and the simulation results.

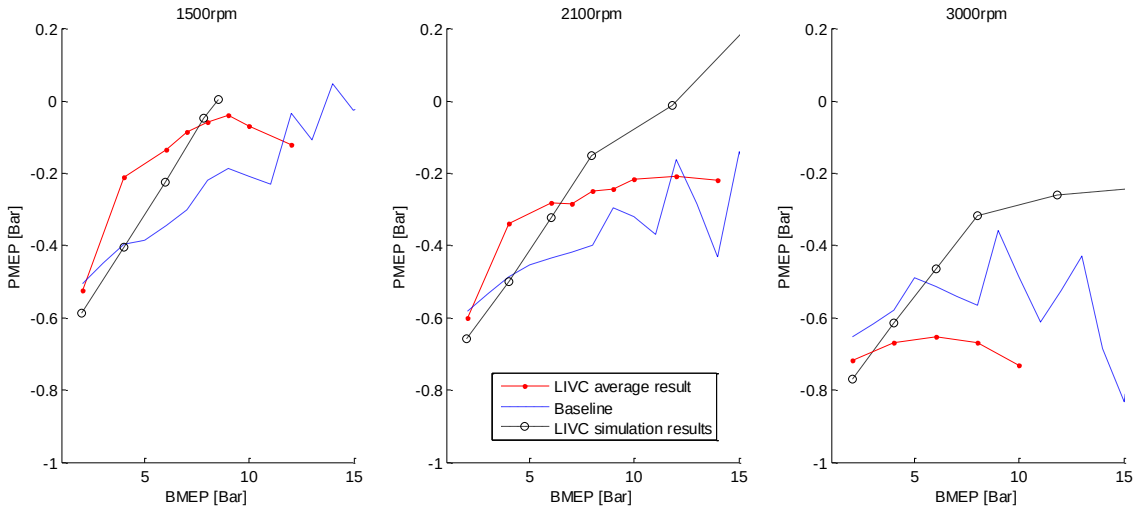

Figure 347 – PMEP of the LIVC-engine at 1500, 2100 and 3000 RPM

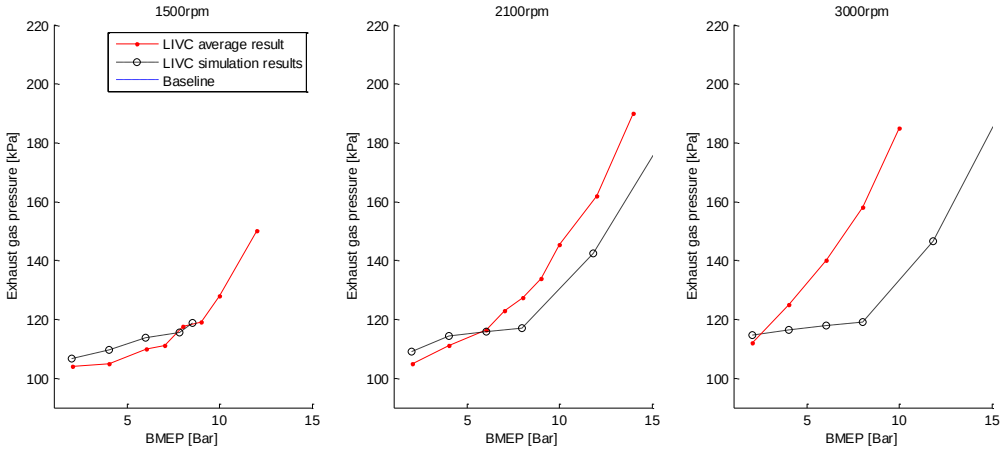

Figure 38 – Exhaust gas pressure for the LIVC-engine

Figure 38 shows how the back pressure in the exhaust manifold deviates from the simulation results. As can be seen there is a correlation for low engine speeds. But as the engine speed increases, the deviation from the simulation results becomes larger and larger. In *figure 39*, intake manifold pressure, exhaust manifold pressure and boost pressure are compared for the different engine speeds. For all engine speeds the boost and exhaust pressure are very close and at 1500 RPM and 2100 RPM there is a pressure drop over the throttle of about 5 kPa when the intake pressure is above atmospheric. For 3000 RPM the pressure drop between boost pressure and manifold pressure is about 30 kPa for all loads.

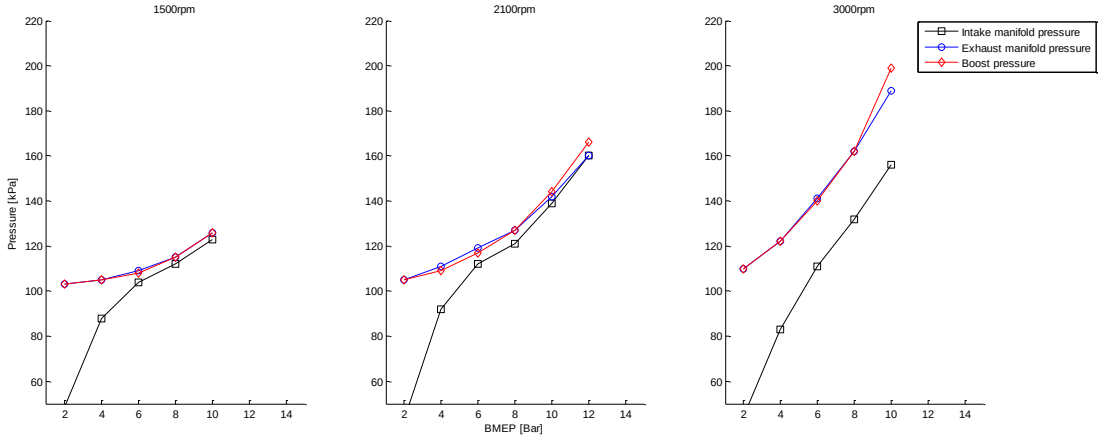

Figure 39 – MAP, boost pressure and exhaust gas pressure. Showing a larger pressure drop over the throttle at 3000 RPM

The maximum torque was measured to 307 Nm at 2100 RPM for the LIVC-engine while the baseline engine produced 374 Nm. Although be with different fuel this is a reduction of 17.8%. The maximum torque measured for the two engines can be seen in *figure 40*.

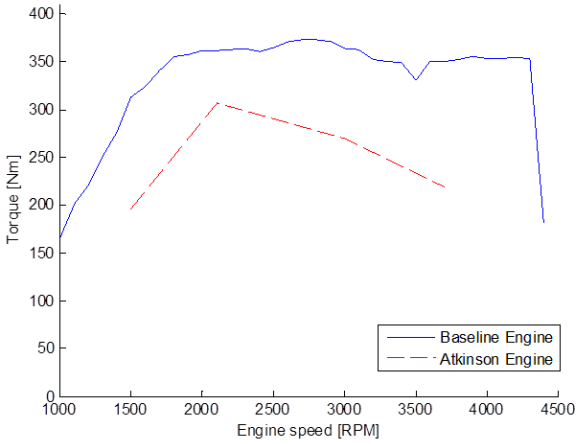

Figure 40 – Maximum torque comparison of the original and LIVC-engine

Figure 41 shows the burn duration from 10-90% mass fraction burnt. As can be seen there is a large deviation from the simulated values while there is a correlation between the LIVC-engine and the test results of the baseline engine. The load point where the burn duration of the LIVC-engine starts to increase compared to the baseline engine, corresponds to the point where the combustion is limited by knock and the ignition has to be retarded. What should also be noticed is the shorter burn durations for the LIVC-engine for the lower load range at 3000 RPM.

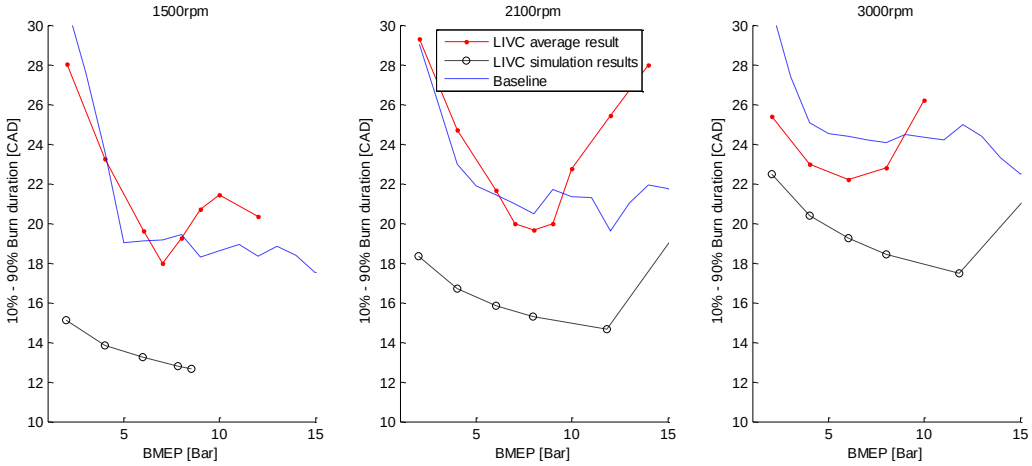

Figure 41 – Burn duration [CAD] from 10-90% mass fraction burnt

5. Discussion

This section provides a discussion around the results of both the simulations and the engine tests. Differences between the engine tests of the baseline and LIVC-engine is discussed as well as differences between the engine tests and the simulation results.

5.1 Simulations

The simulations of the baseline model were performed on a model supplied by VCC. This model is calibrated based on data obtained from CFD simulations as well as physical tests in VCC's test facilities. The baseline model was therefore assumed to provide fairly accurate output data, although it had to be slightly modified to be able to handle part load operation and the lift curves of the LIVC-engine. Furthermore, the GT-power model had been calibrated for full load and might therefore fail to provide accurate predictions at part load. The results of the baseline simulation show a minimum BSFC of 225.2 g/kWh, which is very low compared to the lowest measured BFSC obtained from VCC's test rig. It is also very unlikely that this is the optimum point which suggests that even higher efficiencies could be obtained from simulations. Very low BSFC values were also obtained from the simulations of the LIVC-engine where the lowest observed BSFC was 216.5 g/kWh. One theory to why the simulated BSFC-values deviates from the values obtained from the experimental results can be found in the burn duration, see *figure 41*. When comparing the burn durations from the simulations with the durations from the experimental results, one sees that the simulated burn duration is significantly shorter than they are in the real engine. Longer burn duration suggests a slower burn rate which means that the efficiency values in GT-power are over-estimated. This is probably a result of that the model was calibrated for high loads as previously mentioned.

Since only minor changes were applied to the model in order to implement LIVC, it is believed that the relative comparison between the baseline and LIVC-engine is fairly accurate. The trends observed for how the efficiency changes with various intake cam durations (different IVCs) and lifts were therefore assumed to be accurate. The efficiency appears to increase up to a BMEP of 12 bar but this is not necessarily true since it depends on the resolution of the load map. The load points used for the simulations were set so that the resolution of the load map is higher for the lower load region since this was where LIVC had its greatest potential for efficiency improvements.

When comparing various CRs, the changes to the combustion chamber due to changed piston geometry, was not considered in the simulations. This imposes a source of error since the increased surface to volume ratio, especially at TDC, suggests that the simulated heat transfer might be underestimated. This was not considered to be a major issue since the effective CR with LIVC is heavily reduced from the geometric CR. But also since previous research performed by Heywood et. al [17] proved that efficiency increases up to a geometric CR of 14:1-15:1, although this applied to a conventional Otto-engine.

The simulation results for EGTs suggest very high temperatures throughout the entire load map. This was the case for both the baseline and LIVC-engine and it indicates that something

could be wrong within the heat transfer models in GT-power. However, this has not been concluded. It could also be a consequence of the implementation of a throttle control for part load operation for the same reason as previously discussed. However, there was a trend observed showing that EGTs decreases with LIVC as could be expected due to the over-expansion. Therefore the relative comparison between the baseline and LIVC-engine model was assumed to be fairly accurate.

Unfortunately there is no maximum torque curve provided with the simulation results. The load was controlled in GT-power by setting a target value for the BMEP and to achieve maximum torque a target value equal to the maximum torque of the baseline engine was set. This was done in order to make sure that the target value was higher than the maximum possible torque. Since the target value was much higher than the maximum torque of the LIVC-engine, it resulted in non-converged simulations for the maximum load points. The reason for this was that the wastegate control did not converge properly, which meant that the compressor side of the turbocharger was operating outside the compressor map. This suggested that the target BMEP for maximum load had to be iterated until convergence which required an excessive amount of time. This is the reason why no maximum torque curve could be provided with the simulation results. The presented load maps were however realized with target values set so that the simulations converged. So they should however provide a fair approximation.

5.2 Engine tests

The results from the physical testing show that there is an efficiency improvement at low engine speeds (1500 -2100 RPM) and BMEPs up to 9-10 bar. This was expected based on the simulation results although the simulations suggested improvements also for higher loads. However, the efficiency improvements are not as high as the simulations suggests. Another thing that is realized from the test results is that the simulated efficiency improvements for 3000 rpm do not correlate with the efficiencies calculated from the measured data. One can notice that the deviation from the simulated data increases with increased engine speed. One reason for this is believed to be that the back pressure in the exhaust manifold is higher than what the simulations suggests, see *figure 38*. As a consequence, the pumping losses over the exhaust side increases which could also be observed in *figure 37*. The reason for the high back pressures could be realized by studying *figure 39*. As can be seen the boost pressure provided by the turbocharger at 3000 rpm is a lot higher than the intake manifold pressure. This suggests that there is a pressure drop over the throttle which means that a part of the work performed by the turbine is lost over the throttle. The reason for this is that both the throttle and wastegate are controlled by algorithms in the ECU. The driver only requests a certain load and since the throttle angle is set by the ECU, the behavior observed in *figure 39* occurs. One can take control over the throttle to reduce these effects but unfortunately the amount of time available for testing was limited and therefore this was never further investigated.

A major source of error lies within the comparison of data between the baseline tests performed on VCC and the LIVC-engine tests performed in the test facilities at Chalmers University of Technology. Differences in ambient conditions affect the volumetric efficiency

which in turn affects the BSFC. Also since different measuring equipment is used for the baseline tests from VCC and the LIVC-engine tests, it introduces a source of error. VCC also used RON 98 fuel for their tests while the LIVC-engine was tested with RON 95. This affects the knock limit which is a reason why MBT-timing was only reached for BMEPs up to 8 bar which of course affects the efficiency at higher loads. Also one could suspect that the low valve lift of the LIVC-engine limits the valve flow more than the simulations suggested. This would explain the engine speed dependency since a restricted valve flow would be more evident as the engine speed increases. This would effectively result in less charge being pushed back into the intake manifold and consequently, the effective CR would then be higher than expected. It would then give both increased knock propensity as well as increased pumping losses over the valves. Since the model had previously not been used for the purpose of investigating LIVC, inaccuracies caused by wrongly calibrated reverse discharge coefficients would not have been previously discovered which could be a reason for why the simulations underestimates the flow restriction across the valves. This is however based solely on speculations since it has not been confirmed as a reason for the BSFC's engine speed dependency. Furthermore since the baseline data comes from VCC the VVT settings and the tuning of other parameters are likely to be more optimized compared to the tuning of the LIVC-engine which further affects the relative comparison between the baseline and the LIVC-engine. A baseline test from the same engine test rig would eliminate error sources due to different measuring equipment but also due to differences regarding the test procedure since the tests would have been performed using similar methods in both cases.

The maximum torque curves show that the torque peaks at a lower load compared to the baseline engine, as was expected as an effect of LIVC due to the low trapped volume and boost pressure limitations. However, a rapid torque decrease after 2100 RPM could also be seen in *figure 40*. This effect was not expected based on the simulation results. The reason for this is believed to be the size of the turbocharger. The smaller LP-turbo provides high pressure ratios at relatively low mass flows. But at higher engine speed, it could not provide the pressure ratio required to obtain high loads which limit the maximum torque curve. To avoid this torque drop, a two-stage solution for the boost system could be preferable.

6. Conclusions

- A comparison of the simulated results for the baseline engine and the LIVC-engine pointed toward BSFC-reductions of 7-8% for a major part of the load map.
- A part of the simulated efficiency improvement can be derived from decreased pumping losses. PMEP decreased for a major part of the load map and reductions with up to 60% was observed from the simulations.
- Experimental results from engine tests confirmed the trends shown by the simulations through a comparison between the baseline engine and the LIVC-engine. The BSFC-reduction obtained in reality was however lower than what simulations suggested. BSFC-reductions of 4-6% were obtained for 1500 RPM and BMEPs up to 8 bar. For 2100 RPM and BMEPs up to 9 bar, BSFC-reductions of 2-3% was observed.
- For 3000 rpm and higher, an increase of BSFC was observed, presumably due to high PMEPs caused by high exhaust back pressures from the turbocharger.
- The maximum torque curve was reduced with around 18-40% for the tested engine speeds.

7. References

[1] Martins J.J.G, Uzuneanu K., Ribeiro B.S and Jasasky O. "Thermodynamic Analysis of an Over-Expanded Engine", SAE Technical Paper 2004-01-0617

[2] Heywood J.B, "Internal Combustion Engine Fundamentals", McGraw-Hill Book Co, ISBN 0-07-100499-8, 1988

[3] Taylor J., Fraser N., Dingelstadt R. and Hoffmann H., "Benefits of Late Inlet Valve Timing Strategies Afforded Through the Use of Intake Cam In Cam Applied to a Gasoline Turbocharged Downsized Engine", SAE Technincal Paper 2011-01-0360

[4] Boretti A. and Scalzo J., "Exploring the Advantages of Atkinson Effects in Variable Compression Ratio Turbo GDI Engines", SAE Technical Paper 2011-01-0367

[5] Pertl P., Trattner A., Abis A., Schmidt S., Kirchberger R. and Sato T., "Expansion to Higher Efficiency – Investigations of the Atkinson Cycle in Small Combustion Engines", SAE Technical Paper 2012-32-0059

[6] Atkinson J., "Gas-Engine", U.S. Patent 367496, Aug. 1887

[7] Kobayashi A., Satou T., Isaji H., Takahashi S. and Miyamoto T., "Development of New I3 1.2L Supercharged Gasoline Engine", SAE Technical Paper 2012-01-0415

[8] Miller R., "Supercharged engine", U.S. Patent US2817322 A, Dec. 1957

[9] Austin W.M.,"Variable stroke through use of planetary gear set between connecting rod and crankshaft", U.S. Patent US1278563 A, Sep. 1918

[10] Cady C.P., "Internal-combustion engine", U.S. Patent US1786423 A, Dec. 1930

[11] Honda Motor Co Ltd., "Vaiable stroke engine", EU Patent EP2048335 B1, Feb. 2011

[12] Honda ExLink (Extended Expansion Linkage Engine), http://world.honda.com/powerproducts-technology/exlink/

[13] Holmer E., AB Volvo, "Method for controlling the working cycle of an internal combustion engine", U.S. Patent US4815423 A, Mar. 1989

[14] Mazda Skyactiv-G, http://www.popularmechanics.com/cars/news/fuel-economy/mazda-sky-engine

[15] Choshi M., Asanomi K., Abe H., Okamoto S., Shoji M., "Development of V6 Miller cycle engine",1994, JSAE Review 15 (1994) p.195-200

[16] Gamma Technologies, "GT-Suite Flow Theory Manual", 2012

[17] Ferrán A. Ayala, Michael D. Gerty, John B. Heywood, "Effects of combustion phasing Relative Air-Fuel Ratio, Compression Ratio, and Load on SI-Engine Efficiency", SAE Technical paper 2006-01-0229

[18] Rajput R.K., "Internal combustion engines", Laxmi Publications, ISBN: 817008637X, 2005

Appendix A. Official engine data

OFFICIAL DATA FOR S60	
Issue: 1	
Applicable for :	S60
ENGINES	**B4204T12**
Engine code (rear emblem):	26 (T5)
SoP week	13w46
Emission level EU / US:	PZEV
CYLINDERS (number)	4
DISPLACEMENT (cm3 / cu.in)	1969 / 120,2
BORE (mm / inch)	82 / 3,27
STROKE (mm / inch)	93,2 / 3,67
VALVES (number)	16
DOHC/SOHC	DOHC
COMPRESSION RATIO	10.8:1
FIRING ORDER	1 - 3 - 4 – 2
IDLE SPEED (rpm)	875 – 950
MAX ENGINE SPEED (rpm)	6000
Overrev. / duration	6300 (<3 sec)
MAX ENGINE POWER (kW / rps)	179 / 93
(metric hp / rpm)	NA
(English hp / rpm)	240 / 5600
MAX ENGINE RATED POWER (kW / rps)	
(for China authority submission) (hp / rpm)	
MAX ENGINE TORQUE (Nm / rps)	350 / 25 – 75
(kpm / rpm)	35,7 / 1500-4500
(ft.lbf / rpm)	258 / 1500-4500
NB:	Power and torque measured according to EEC 80/1269*1999/99 & ECE R85-00.

Appendix B. Testing results, Emissions

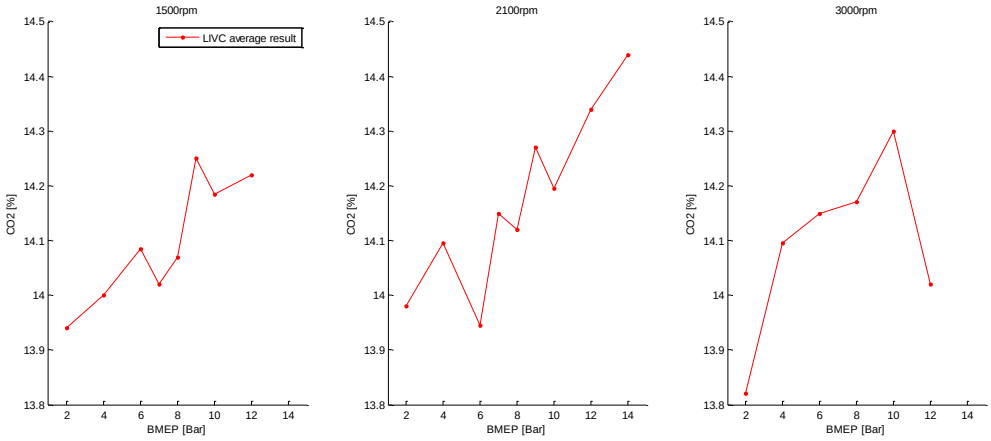

Figure 42 – CO_2-emissions, measured before catalyst and presented as an average value of all measures for each load

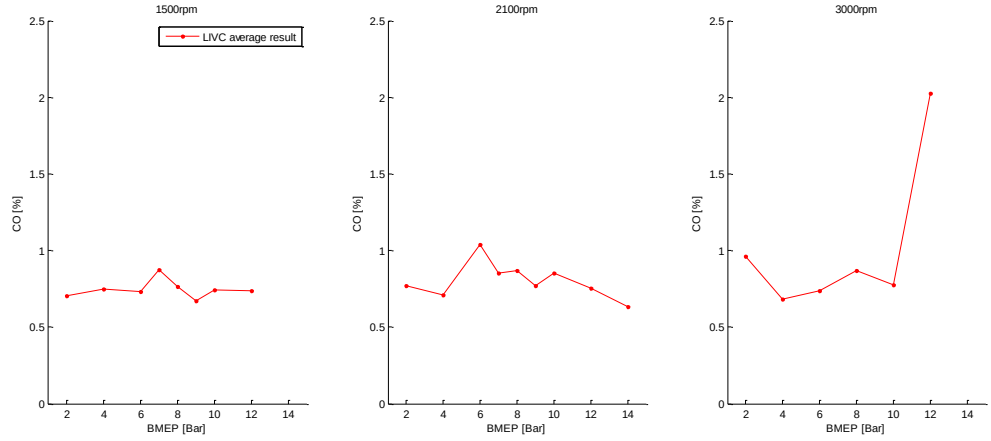

Figure 43 – CO-emissions, measured before catalyst and presented as an average value of all measures for each load

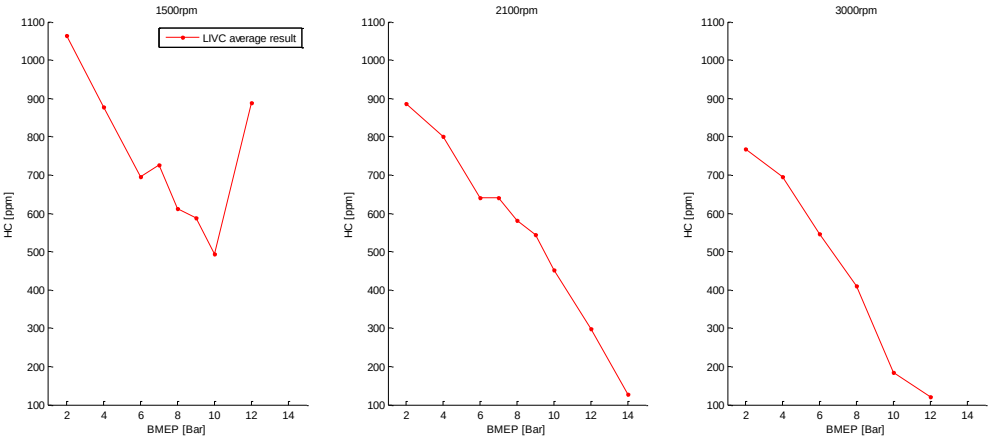

Figure 44 – HC-emissions, measured before catalyst and presented as an average value of all measures for each load

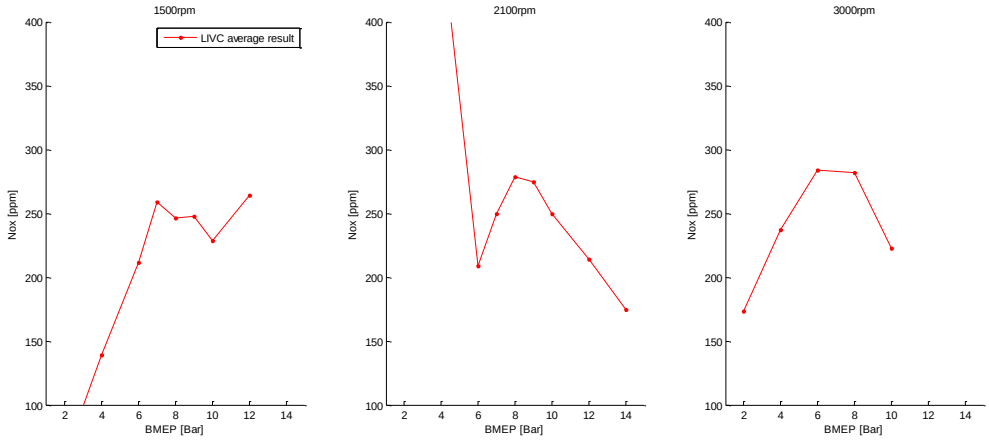

Figure 45 – NOx-emissions, measured before catalyst and presented as an average value of all measures for each load